

**Rare decays  $B_u^+ \rightarrow \pi^+ \ell^+ \ell^-$ ,  $\rho^+ \ell^+ \ell^-$  and  $B_d^0 \rightarrow \ell^+ \ell^-$  in the  $R$ -parity violating supersymmetry**Jian-Jun Wang,<sup>1,2</sup> Ru-Min Wang,<sup>3</sup> Yuan-Guo Xu,<sup>1</sup> and Ya-Dong Yang<sup>1,\*</sup><sup>1</sup>*Institute of Particle Physics, Huazhong Normal University, Wuhan, Hubei 430079, P. R. China*<sup>2</sup>*Department of Physics, Henan Normal University, XinXiang, Henan 453007, P. R. China*<sup>3</sup>*Department of Physics, Yonsei University, Seoul 120-479, Korea*

(Received 5 November 2007; published 22 January 2008)

We study the rare decays  $B_u^+ \rightarrow \pi^+ \ell^+ \ell^-$ ,  $\rho^+ \ell^+ \ell^-$  and  $B_d^0 \rightarrow \ell^+ \ell^-$  ( $\ell = e, \mu$ ) in the  $R$ -parity violating supersymmetric standard model. From the latest upper limits of  $\mathcal{B}(B_u^+ \rightarrow \pi^+ \ell^+ \ell^-)$  and  $\mathcal{B}(B_d^0 \rightarrow \ell^+ \ell^-)$ , we have derived new upper bounds on the relevant  $R$ -parity violating couplings products, which are stronger than the existing ones. Using the constrained parameter space, we present the  $R$ -parity violating effects on the branching ratios and the forward-backward asymmetries of these decays. We find that  $\mathcal{B}(B_d^0 \rightarrow \ell^+ \ell^-)$  and  $\mathcal{B}(B_u^+ \rightarrow \rho^+ \ell^+ \ell^-)$  could be enhanced several orders by the  $R$ -parity violating sneutrino and squark exchanges, respectively. The  $R$ -parity violating effects on the dilepton invariant mass spectra of  $B_u^+ \rightarrow \pi^+ \ell^+ \ell^-$ ,  $\rho^+ \ell^+ \ell^-$  and the normalized forward-backward asymmetry  $\mathcal{A}_{\text{FB}}(B_u^+ \rightarrow \pi^+ \ell^+ \ell^-)$  and  $\mathcal{A}_{\text{FB}}(B_u^+ \rightarrow \rho^+ \ell^+ \ell^-)$  are studied in detail. Our results could be used to probe the  $R$ -parity violating effects and will correlate with searches for the direct  $R$ -parity violating signals at the future experiments.

DOI: [10.1103/PhysRevD.77.014017](https://doi.org/10.1103/PhysRevD.77.014017)

PACS numbers: 13.20.He, 12.15.Ji, 12.15.Mm, 12.60.Jv

**I. INTRODUCTION**

In the standard model (SM), rare  $B$  decays  $B_u^+ \rightarrow \pi^+ \ell^+ \ell^-$ ,  $\rho^+ \ell^+ \ell^-$  and  $B_d^0 \rightarrow \ell^+ \ell^-$  ( $\ell = e, \mu$ ) are induced by  $\bar{b} \rightarrow \bar{d} \ell^+ \ell^-$  flavor changing neutral current (FCNC) and expected to be highly suppressed. These decays could be an important testing ground of the SM and offer a complementary means to search for new physics by probing the indirect effects of new interactions.

The physical aspects of these decays are similar to the  $b \rightarrow s \ell^+ \ell^-$  decays, which, due to its much larger rates, have been studied much more extensively in the SM [1–4] and its various extensions [5–10]. In addition to the  $b \rightarrow s \ell^+ \ell^-$  decays, the  $b \rightarrow d \ell^+ \ell^-$  decays would serve an independent test for new flavor changing interactions. Experimental progresses aimed to such semileptonic FCNC decays have been made by BABAR [11] and Belle [12] with the measurements of the forward-backward asymmetry ( $\mathcal{A}_{\text{FB}}$ ) of  $B \rightarrow K^* \ell^+ \ell^-$  and the branching ratios of both  $B \rightarrow K^* \ell^+ \ell^-$  and  $K \ell^+ \ell^-$ . Furthermore, the radiative  $b \rightarrow d \gamma$  penguin processes  $B \rightarrow \rho \gamma$  and  $\omega \gamma$  have been measured by BABAR [13] and Belle [14]. Along with these progresses, BABAR, Belle and CDF have begun to probe  $b \rightarrow d \ell^+ \ell^-$  decays. Recently, BABAR has made a search for  $B \rightarrow \pi \ell^+ \ell^-$  and  $B_d^0 \rightarrow \ell^+ \ell^-$  decays [15]. It is interesting to note that the new upper limit of  $\mathcal{B}(B \rightarrow \pi \ell^+ \ell^-) < 9.1 \times 10^{-8}$  at 90% C.L. [15] has improved the previous upper limits [16] by 4 orders of magnitude. Meanwhile, the upper limit of  $\mathcal{B}(B_d^0 \rightarrow \mu^+ \mu^-)$  has been improved to be  $\mathcal{B}(B_d^0 \rightarrow \mu^+ \mu^-) < 1.5 \times 10^{-8}$  at 90% C.L. by CDF [17]. These renewed upper limits from

BABAR [15] and CDF [17] will provide powerful constraints on new physics.

In the literature, many useful observables in  $B \rightarrow \rho \ell^+ \ell^-$  and  $B \rightarrow \pi \ell^+ \ell^-$  decays, such as branching ratio,  $CP$ -asymmetry, forward-backward asymmetry etc., have been investigated in the framework of the SM [18], the two Higgs doublet models [19–21] and supersymmetry models (SUSY) [22]. With the new upper limits, it would be very worthy to study these decays in other new physics models to derive bounds on the relevant parameters.

In this paper, we will study these decays in the  $R$ -parity violating (RPV) supersymmetric standard model [23–25]. The phenomenological constraints on the RPV couplings have been studied extensively in  $B$  decays [26]. At first, we will update the SM expectations of these decays with the up-to-date inputs, such as the new light-cone QCD sum rules results for  $B \rightarrow \pi(\rho)$  form factors [27] and the electroweak parameters [28]. To make realistic estimations, we have taken into account of the uncertainties of the input parameters by varying them randomly within  $1\sigma$  variance.

The decays  $B_u^+ \rightarrow \rho^+ \ell^+ \ell^-$ ,  $B_u^+ \rightarrow \pi^+ \ell^+ \ell^-$ , and  $B_d^0 \rightarrow \ell^+ \ell^-$  are all induced at the parton level by the same set of the RPV coupling products in the RPV SUSY. From the latest experimental data and the theoretical parameters, we will derive the new upper limits on the relevant RPV coupling products. Then we will use the constrained parameter space to predict the RPV effects on the branching ratios of  $B_u^+ \rightarrow \rho^+ \ell^+ \ell^-$ ,  $B_u^+ \rightarrow \pi^+ \ell^+ \ell^-$ , and  $B_d^0 \rightarrow \ell^+ \ell^-$  decays, and the forward-backward asymmetries of  $B_u^+ \rightarrow \rho^+ \ell^+ \ell^-$  and  $B_u^+ \rightarrow \pi^+ \ell^+ \ell^-$ . Moreover, we will compare the SM predictions with the RPV predictions about the dilepton invariant mass spectra and the normalized forward-backward asymmetries in  $B_u^+ \rightarrow \rho^+ \ell^+ \ell^-$  and  $B_u^+ \rightarrow \pi^+ \ell^+ \ell^-$  decays.

\*Corresponding author  
yangyd@iopp.ccnu.edu.cn

The paper is organized as follows. In Sec. II, we derive the expressions for  $B_u^+ \rightarrow \rho^+ \ell^+ \ell^-$ ,  $B_u^+ \rightarrow \pi^+ \ell^+ \ell^-$ , and  $B_d^0 \rightarrow \ell^+ \ell^-$  processes in the RPV SUSY. In Sec. III, our numerical analyses are presented. We display the constrained parameter spaces which satisfy all the upper limits of  $\mathcal{B}(B_u^+ \rightarrow \pi^+ \ell^+ \ell^-)$  and  $\mathcal{B}(B_d^0 \rightarrow \ell^+ \ell^-)$ , and then we use the constrained parameter spaces to present the RPV effects on  $\mathcal{A}_{\text{FB}}(B_u^+ \rightarrow \rho^+ \ell^+ \ell^-)$ ,  $\mathcal{A}_{\text{FB}}(B_u^+ \rightarrow \pi^+ \ell^+ \ell^-)$ ,  $\mathcal{B}(B_u^+ \rightarrow \pi^+ \ell^+ \ell^-)$ ,  $\mathcal{B}(B_u^+ \rightarrow \rho^+ \ell^+ \ell^-)$ , and  $\mathcal{B}(B_d^0 \rightarrow \ell^+ \ell^-)$ . We also show the RPV effects on the dilepton invariant mass spectra and the normalized forward-backward asymmetries in  $B_u^+ \rightarrow \rho^+ \ell^+ \ell^-$  and  $B_u^+ \rightarrow \pi^+ \ell^+ \ell^-$  decays. Section IV is devoted to our summary.

## II. THE THEORETICAL FRAME FOR $B_u^+ \rightarrow \pi^+ \ell^+ \ell^-$ , $B_u^+ \rightarrow \rho^+ \ell^+ \ell^-$ AND $B_d^0 \rightarrow \ell^+ \ell^-$

### A. The decay branching ratios in the SM

#### 1. The semileptonic decays $B^+ \rightarrow \pi^+ \ell^+ \ell^-$ and $B^+ \rightarrow \rho^+ \ell^+ \ell^-$

In the SM, the effective Hamiltonian for the  $\bar{b} \rightarrow \bar{d} \ell^+ \ell^-$  decay can be written as [3,29,30]

$$\mathcal{H}_{\text{eff}}^{\text{SM}} = -\frac{4G_F}{\sqrt{2}} V_{td} V_{tb}^* \left\{ \sum_{i=1}^{10} C_i(\mu) \mathcal{O}_i(\mu) + \lambda_u^* \sum_{i=1}^2 C_i(\mu) [\mathcal{O}_i(\mu) - \mathcal{O}_i^{(u)}(\mu)] \right\}, \quad (1)$$

where  $\lambda_u^* \equiv \frac{V_{ub}^* V_{ud}}{V_{tb}^* V_{td}}$ . The explicit form of all operators  $\mathcal{O}_i(\mu)$  and the Wilson coefficients  $C_i(\mu)$  calculated in the naive dimensional regularization (NDR) scheme can be found in [3]. The effective Hamiltonian leads the QCD corrected matrix element for  $\bar{b} \rightarrow \bar{d} \ell^+ \ell^-$  [3,29]

$$\begin{aligned} \mathcal{M}^{\text{SM}}(\bar{b} \rightarrow \bar{d} \ell^+ \ell^-) &= \frac{G_F \alpha_e}{\sqrt{2} \pi} V_{tb}^* V_{td} \left\{ C_9^{\text{eff}}(\bar{b} \gamma_\mu P_L d)(\bar{\ell} \gamma^\mu \ell) \right. \\ &\quad + C_{10}(\bar{b} \gamma_\mu P_L d)(\bar{\ell} \gamma^\mu \gamma_5 \ell) \\ &\quad \left. - 2\hat{m}_b C_7^{\text{eff}} \left( \bar{b} i \sigma_{\mu\nu} \frac{\hat{q}^\nu}{\hat{s}} P_L d \right) (\bar{\ell} \gamma^\mu \ell) \right\}, \end{aligned} \quad (2)$$

with  $P_{L,R} \equiv (1 \mp \gamma_5)/2$ ,  $s = q^2$ , and  $q = p_+ + p_-$  ( $p_\pm$  are the four-momenta of the leptons). We take  $m_d/m_b = 0$ , but keep the leptons mass. The hat denotes normalization in terms of the  $B$ -meson mass,  $m_B$ , e.g.  $\hat{s} = s/m_B^2$ ,  $\hat{m}_q = m_q/m_B$ .

$C_9^{\text{eff}}(\mu)$  contains the one-gluon corrections to  $\mathcal{O}_9$  ( $\omega(\hat{s})$  term) [31] and the corrections of four-quark operators  $\mathcal{O}_{1-6}$  and  $\mathcal{O}_{1,2}^u$  in Eq. (1) [32], which can be written as [29]

$$C_9^{\text{eff}}(\mu) = \xi_1 + \lambda_u^* \xi_2, \quad (3)$$

with

$$\begin{aligned} \xi_1 &= \hat{C}_9^{\text{NDR}} \left[ 1 + \frac{\alpha_s(\mu)}{\pi} \omega(\hat{s}) \right] + g(\hat{m}_c, \hat{s})(3C_1 + C_2 \\ &\quad + 3C_3 + C_4 + 3C_5 + C_6) - \frac{1}{2} g(1, \hat{s})(4C_3 + 4C_4 \\ &\quad + 3C_5 + C_6) - \frac{1}{2} g(0, \hat{s})(C_3 + 3C_4) \\ &\quad + \frac{2}{9}(3C_3 + C_4 + 3C_5 + C_6), \end{aligned} \quad (4)$$

$$\xi_2 = [g(\hat{m}_c, \hat{s}) - g(0, \hat{s})](3C_1 + C_2). \quad (5)$$

In addition to the short distance contributions,  $\bar{b} \rightarrow \bar{d} \ell^+ \ell^-$  decay also receives long distance contributions from both on- and off-shell vector mesons, which can be incorporated in  $C_9^{\text{eff}}$  by the replacement [33,34]

$$g(\hat{m}_c, \hat{s}) \rightarrow g(\hat{m}_c, \hat{s}) - \frac{3\pi}{\alpha_e^2} \sum_{V_i=\psi,\psi',\dots} \kappa \frac{m_{V_i} \Gamma(V_i \rightarrow \ell^+ \ell^-)}{s - m_{V_i}^2 + i\Gamma_{V_i} m_{V_i}}. \quad (6)$$

This issue has been extensively discussed in the literature [35,36].

With these formulas, one can derive the decay amplitudes for  $B^+ \rightarrow \pi^+ \ell^+ \ell^-$  and  $\rho^+ \ell^+ \ell^-$  decays. Recently the form factors for  $B \rightarrow \pi$  and  $B \rightarrow \rho$  transitions have been improved in the framework of light-cone QCD sum rules [27], with one-loop radiative corrections to twist-2 and twist-3 contributions, and leading order twist-4 corrections. Using the form factors defined in [27] and the matrix in Eq. (2), we get the following amplitudes for  $B_u^+ \rightarrow \pi^+ \ell^+ \ell^-$  and  $B_u^+ \rightarrow \rho^+ \ell^+ \ell^-$  decays:

$$\begin{aligned} \mathcal{M}^{\text{SM}}(B \rightarrow M \ell^+ \ell^-) &= \frac{G_F \alpha_e}{2\sqrt{2} \pi} V_{td} V_{tb}^* m_B [\mathcal{T}_{1\mu}(\bar{\ell} \gamma^\mu \ell) \\ &\quad + \mathcal{T}_{2\mu}(\bar{\ell} \gamma^\mu \gamma_5 \ell)], \end{aligned} \quad (7)$$

where for  $B_u^+ \rightarrow \pi^+ \ell^+ \ell^-$ ,

$$\mathcal{T}_{1\mu} = A'(\hat{s}) \hat{p}_\mu + B'(\hat{s}) \hat{q}_\mu, \quad (8)$$

$$\mathcal{T}_{2\mu} = C'(\hat{s}) \hat{p}_\mu + D'(\hat{s}) \hat{q}_\mu, \quad (9)$$

and for  $B_u^+ \rightarrow \rho^+ \ell^+ \ell^-$ ,

$$\begin{aligned} \mathcal{T}_{1\mu} &= A(\hat{s}) \epsilon_{\mu\rho\alpha\beta} \epsilon^{*\rho} \hat{p}_B^\alpha \hat{p}_\rho^\beta - iB(\hat{s}) \epsilon_\mu^* \\ &\quad + iC(\hat{s}) (\epsilon^* \cdot \hat{p}_B) \hat{p}_\mu + iD(\hat{s}) (\epsilon^* \cdot \hat{p}_B) \hat{q}_\mu, \end{aligned} \quad (10)$$

$$\begin{aligned} \mathcal{T}_{2\mu} &= E(\hat{s}) \epsilon_{\mu\rho\alpha\beta} \epsilon^{*\rho} \hat{p}_B^\alpha \hat{p}_\rho^\beta - iF(\hat{s}) \epsilon_\mu^* \\ &\quad + iG(\hat{s}) (\epsilon^* \cdot \hat{p}_B) \hat{p}_\mu + iH(\hat{s}) (\epsilon^* \cdot \hat{p}_B) \hat{q}_\mu, \end{aligned} \quad (11)$$

with  $p \equiv p_B + p_M$  ( $M = \pi^+$  or  $\rho^+$ ).

The auxiliary functions in  $\mathcal{T}_{1,2\mu}$  are defined as [6]

$$A'(\hat{s}) = C_9^{\text{eff}}(\hat{s}) f_+(\hat{s}) + \frac{2\hat{m}_b}{1 + \hat{m}_\pi} C_7^{\text{eff}} f_T(\hat{s}), \quad (12)$$

$$B'(\hat{s}) = C_9^{\text{eff}}(\hat{s})f_-(\hat{s}) - \frac{2\hat{m}_b}{\hat{s}}(1 - \hat{m}_\pi)C_7^{\text{eff}}f_T(\hat{s}), \quad (13)$$

$$C'(\hat{s}) = C_{10}f_+(\hat{s}), \quad (14)$$

$$D'(\hat{s}) = C_{10}f_-(\hat{s}), \quad (15)$$

$$A(\hat{s}) = \frac{2}{1 + \hat{m}_\rho}C_9^{\text{eff}}(\hat{s})V(\hat{s}) + \frac{4\hat{m}_b}{\hat{s}}C_7^{\text{eff}}T_1(\hat{s}), \quad (16)$$

$$B(\hat{s}) = (1 + \hat{m}_\rho) \left[ C_9^{\text{eff}}(\hat{s})A_1(\hat{s}) + \frac{2\hat{m}_b}{\hat{s}}(1 - \hat{m}_\rho)C_7^{\text{eff}}T_2(\hat{s}) \right], \quad (17)$$

$$C(\hat{s}) = \frac{1}{1 - \hat{m}_\rho^2} \left[ (1 - \hat{m}_\rho)C_9^{\text{eff}}(\hat{s})A_2(\hat{s}) + 2\hat{m}_b C_7^{\text{eff}} \left( T_3(\hat{s}) + \frac{1 - \hat{m}_\rho}{\hat{s}} T_2(\hat{s}) \right) \right], \quad (18)$$

$$D(\hat{s}) = \frac{1}{\hat{s}} \left[ C_9^{\text{eff}}(\hat{s})((1 + \hat{m}_\rho)A_1(\hat{s}) - (1 - \hat{m}_\rho)A_2(\hat{s}) - 2\hat{m}_\rho A_0(\hat{s})) - 2\hat{m}_b C_7^{\text{eff}} T_3(\hat{s}) \right], \quad (19)$$

$$E(\hat{s}) = \frac{2}{1 + \hat{m}_\rho} C_{10} V(\hat{s}), \quad (20)$$

$$F(\hat{s}) = (1 + \hat{m}_\rho) C_{10} A_1(\hat{s}), \quad (21)$$

$$G(\hat{s}) = \frac{1}{1 + \hat{m}_\rho} C_{10} A_2(\hat{s}), \quad (22)$$

$$H(\hat{s}) = \frac{1}{\hat{s}} C_{10} [(1 + \hat{m}_\rho)A_1(\hat{s}) - (1 - \hat{m}_\rho)A_2(\hat{s}) - 2\hat{m}_\rho A_0(\hat{s})]. \quad (23)$$

The kinematic variables  $(\hat{s}, \hat{u})$  are chosen to be

$$\hat{s} = \hat{q}^2 = (\hat{p}_+ + \hat{p}_-)^2, \quad (24)$$

$$\hat{u} = (\hat{p}_B - \hat{p}_-)^2 - (\hat{p}_B - \hat{p}_+)^2, \quad (25)$$

which are bounded as

$$(2\hat{m}_\ell)^2 \leq \hat{s} \leq (1 - \hat{m}_\rho)^2, \quad (26)$$

$$-\hat{u}(\hat{s}) \leq \hat{u} \leq \hat{u}(\hat{s}), \quad (27)$$

with  $\hat{m}_\ell = m_\ell/m_B$  and

$$\hat{u}(\hat{s}) = \sqrt{\lambda \left( 1 - 4 \frac{\hat{m}_\ell^2}{\hat{s}} \right)}, \quad (28)$$

$$\lambda \equiv \lambda(1, \hat{m}_{\pi, \rho}^2, \hat{s}) = 1 + \hat{m}_{\pi, \rho}^4 + \hat{s}^2 - 2\hat{s} - 2\hat{m}_{\pi, \rho}^2(1 + \hat{s}). \quad (29)$$

Note that the variable  $\hat{u}$  corresponds to  $\theta$ , the angle between the three-momentum of the  $\ell^+$  lepton and the  $B$  meson in the dilepton center-of-mass system (CMS) frame, through the relation  $\hat{u} = -\hat{u}(s) \cos \theta$  [37]. Keeping the lepton mass, the double differential decay branching ratios  $\mathcal{B}^{\pi^+}$  and  $\mathcal{B}^{\rho^+}$  for the decays  $B_u^+ \rightarrow \pi^+ \ell^+ \ell^-$  and  $B_u^+ \rightarrow \rho^+ \ell^+ \ell^-$ , respectively, are found to be

$$\begin{aligned} \frac{d^2 \mathcal{B}_{\text{SM}}^{\rho^+}}{d\hat{s}d\hat{u}} &= \tau_B \frac{G_F^2 \alpha_e^2 m_B^5}{2^{11} \pi^5} |V_{td} V_{tb}^*|^2 \{ (|A|^2 + |C|^2)(\lambda - \hat{u}^2) \\ &+ |C|^2 4\hat{m}_\ell^2 (2 + 2\hat{m}_{\pi^+}^2 - \hat{s}) \\ &+ \text{Re}(C'D'^*) 8\hat{m}_\ell^2 (1 - \hat{m}_{\pi^+}^2) + |D'|^2 4\hat{m}_\ell^2 \hat{s} \}, \end{aligned} \quad (30)$$

$$\begin{aligned} \frac{d^2 \mathcal{B}_{\text{SM}}^{\pi^+}}{d\hat{s}d\hat{u}} &= \tau_B \frac{G_F^2 \alpha_e^2 m_B^5}{2^{11} \pi^5} |V_{td} V_{tb}^*|^2 \left\{ \frac{|A|^2}{4} (\hat{s}(\lambda + \hat{u}^2) + 4\hat{m}_\ell^2 \lambda) + \frac{|E|^2}{4} (\hat{s}(\lambda + \hat{u}^2) - 4\hat{m}_\ell^2 \lambda) \right. \\ &+ \frac{1}{4\hat{m}_{\rho^+}^2} [ |B|^2 (\lambda - \hat{u}^2 + 8\hat{m}_{\rho^+}^2 (\hat{s} + 2\hat{m}_\ell^2)) + |F|^2 (\lambda - \hat{u}^2 + 8\hat{m}_{\rho^+}^2 (\hat{s} - 4\hat{m}_\ell^2)) ] - 2\hat{s} \hat{u} [\text{Re}(BE^*) + \text{Re}(AF^*)] \\ &+ \frac{\lambda}{4\hat{m}_{\rho^+}^2} [ |C|^2 (\lambda - \hat{u}^2) + |G|^2 (\lambda - \hat{u}^2 + 4\hat{m}_\ell^2 (2 + 2\hat{m}_{\rho^+}^2 - \hat{s})) ] - \frac{1}{2\hat{m}_{\rho^+}^2} [\text{Re}(BC^*) (1 - \hat{m}_{\rho^+}^2 - \hat{s}) (\lambda - \hat{u}^2) \\ &+ \text{Re}(FG^*) ((1 - \hat{m}_{\rho^+}^2 - \hat{s}) (\lambda - \hat{u}^2) + 4\hat{m}_\ell^2 \lambda) ] - 2 \frac{\hat{m}_\ell^2}{\hat{m}_{\rho^+}^2} \lambda [\text{Re}(FH^*) - \text{Re}(GH^*) (1 - \hat{m}_{\rho^+}^2)] + |H|^2 \frac{\hat{m}_\ell^2}{\hat{m}_{\rho^+}^2} \hat{s} \lambda \left. \right\}. \end{aligned} \quad (31)$$

## 2. The pure leptonic decays $B_d^0 \rightarrow \ell^+ \ell^-$

In the SM, the purely leptonic decays  $B_d^0 \rightarrow \ell^+ \ell^-$  proceed through electroweak penguin diagrams with  $Z$  exchange as well as  $W$  box diagrams. The photon penguin contribution is forbidden by the conservation of electromagnetic current. The

effective Hamiltonian for these decays is [38]

$$\mathcal{H}_{\text{eff}}^{\text{SM}}(B_d^0 \rightarrow \ell^+ \ell^-) = -\frac{G_F}{\sqrt{2}} \frac{\alpha_e}{2\pi \sin^2 \theta_W} \times V_{td} V_{tb}^* Y(x_t) (\bar{b}d)_{V-A} (\bar{\ell}\ell)_{V-A}, \quad (32)$$

where  $x_t \equiv m_t^2/m_W^2$ , which leads to the branching ratio

$$\begin{aligned} \mathcal{B}^{\text{SM}}(B_d \rightarrow \ell^+ \ell^-) &= \frac{\tau_{B_d}}{16\pi m_{B_d}} \sqrt{1 - 4\hat{m}_\ell^2} \\ &\times |\mathcal{M}^{\text{SM}}(B_d \rightarrow \ell^+ \ell^-)|^2 \\ &= \tau_{B_d} \frac{G_F^2}{\pi} \left( \frac{\alpha_e}{4\pi \sin^2 \theta_W} \right)^2 f_{B_d}^2 m_\ell^2 m_{B_d} \\ &\times \sqrt{1 - 4\hat{m}_\ell^2} |V_{td} V_{tb}^*|^2 |Y(x_t)|^2. \end{aligned} \quad (33)$$

In the SM, as shown by Eq. (33), the decays are suppressed by helicity conservation (the factor  $m_\ell^2/m_B^2$ ) in addition to the small  $V_{td}$ . However, they are very sensitive to new physics with pseudoscalar interactions.

### B. The decay amplitudes in the RPV SUSY

In the most general superpotential of the minimal supersymmetric standard model, the RPV superpotential is given by [23–25]

$$\begin{aligned} \mathcal{W}_{\mathcal{R}_p} &= \mu_i \hat{L}_i \hat{H}_u + \frac{1}{2} \lambda_{[ijk]} \hat{L}_i \hat{L}_j \hat{E}_k^c + \lambda'_{ijk} \hat{L}_i \hat{Q}_j \hat{D}_k^c \\ &+ \frac{1}{2} \lambda''_{[ijk]} \hat{U}_i^c \hat{D}_j^c \hat{D}_k^c, \end{aligned} \quad (34)$$

where  $i, j, k = 1, 2, 3$  are generation indices and  $c$  denotes a charge conjugate field.  $\hat{L}_i(\hat{Q}_i)$  are the lepton(quark)  $SU(2)_L$  doublet superfields,  $\hat{E}_k^c$ ,  $\hat{U}_i^c$ , and  $\hat{D}_k^c$  are the singlet superfields, respectively. The bilinear RPV superpotential terms  $\mu_i \hat{L}_i \hat{H}_u$  can be rotated away by suitable redefining the lepton and Higgs superfields [25]. However, the rotation will generate a soft SUSY breaking bilinear term which would affect our calculation through penguin level. The processes discussed in this paper could be induced by the tree-level RPV couplings, so that we would neglect subleading RPV penguin contributions in this study. The  $\lambda$  and  $\lambda'$  couplings in Eq. (34) break the lepton number, while the  $\lambda''$  couplings break the baryon number. There are 27  $\lambda'_{ijk}$  couplings, 9  $\lambda_{ijk}$ , and 9  $\lambda''_{ijk}$  couplings.  $\lambda_{[ijk]}$  are antisymmetric with respect to their first two indices, and  $\lambda''_{[ijk]}$  are antisymmetric with  $j$  and  $k$ . All the processes considered in this paper involve terms in the RPV Hamiltonian with two leptons and two quarks as external fields. From Eq. (34), the Hamiltonian of  $\bar{b} \rightarrow \bar{d} \ell^+ \ell^-$  process due to the squarks and sneutrinos exchange are

$$\begin{aligned} \mathcal{H}_{\text{eff}}^{\mathcal{R}_p} &= -\frac{1}{2} \sum_i \frac{\lambda'_{ijk} \lambda_{lin}^*}{m_{\tilde{u}_{iL}}^2} (\bar{d}_k \gamma^\mu P_R d_n) (\bar{\ell}_l \gamma_\mu P_L \ell_j) \\ &+ \sum_i \left\{ \frac{\lambda_{ijk} \lambda_{imn}^*}{m_{\tilde{v}_{iL}}^2} (\bar{d}_m P_R d_n) (\bar{\ell}_k P_L \ell_j) \right. \\ &\left. + \frac{\lambda'_{ijk} \lambda'_{imn}}{m_{\tilde{v}_{iL}}^2} (\bar{d}_n P_L d_m) (\bar{\ell}_j P_R \ell_k) \right\}. \end{aligned} \quad (35)$$

The RPV Feynman diagrams of  $B_u^+ \rightarrow \pi^+ \ell^+ \ell^-$ ,  $B_u^+ \rightarrow \rho^+ \ell^+ \ell^-$ , and  $B_d^0 \rightarrow \ell^+ \ell^-$  are displayed in Figs. 1 and 2, respectively.

From Eq. (35), we can obtain the RPV decay amplitude for  $B_u^+ \rightarrow \pi^+ \ell^+ \ell^-$

$$\begin{aligned} \mathcal{M}^{\mathcal{R}_p}(B_u^+ \rightarrow \pi^+ \ell^+ \ell^-) &= Y_{\tilde{u}} (\bar{\ell}_k (\not{p}_B + \not{p}_{\pi^+}) (1 - \gamma_5) \ell_j) \\ &+ Y_{\tilde{v}} (\bar{\ell}_k (1 - \gamma_5) \ell_j) \\ &+ Y'_{\tilde{v}} (\bar{\ell}_k (1 + \gamma_5) \ell_j), \end{aligned} \quad (36)$$

where

$$Y_{\tilde{u}} = -\sum_i \frac{\lambda'_{ji3} \lambda_{ki1}^*}{8m_{\tilde{u}_{iL}}^2} f_{+}^{B_u^+ \rightarrow \pi^+}(\hat{s}), \quad (37)$$

$$Y_{\tilde{v}} = \sum_i \frac{\lambda_{ijk} \lambda_{i31}^*}{4m_{\tilde{v}_{iL}}^2} f_{+}^{B_u^+ \rightarrow \pi^+}(\hat{s}) \frac{m_B^2 - m_{\pi^+}^2}{\bar{m}_b - \bar{m}_d}, \quad (38)$$

$$Y'_{\tilde{v}} = \sum_i \frac{\lambda'_{ikj} \lambda'_{i13}}{4m_{\tilde{v}_{iL}}^2} f_{+}^{B_u^+ \rightarrow \pi^+}(\hat{s}) \frac{m_B^2 - m_{\pi^+}^2}{\bar{m}_b - \bar{m}_d}, \quad (39)$$

with  $\bar{m}_b$  and  $\bar{m}_d$  are the quark's running masses at the scale  $m_b$ .

For  $B_u^+ \rightarrow \rho^+ \ell^+ \ell^-$ , the RPV amplitude is

$$\begin{aligned} \mathcal{M}^{\mathcal{R}_p}(B_u^+ \rightarrow \rho^+ \ell^+ \ell^-) &= \mathcal{T}_{3\mu} (\bar{\ell}_k \gamma^\mu (1 - \gamma_5) \ell_j) \\ &+ \Phi_{\tilde{v}} (\bar{\ell}_k (1 - \gamma_5) \ell_j) \\ &+ \Phi'_{\tilde{v}} (\bar{\ell}_k (1 + \gamma_5) \ell_j), \end{aligned} \quad (40)$$

where

$$\begin{aligned} \mathcal{T}_{3\mu} &= I(\hat{s}) \epsilon_{\mu\rho\alpha\beta} \epsilon^{*\rho} \hat{p}_B^\alpha \hat{p}_{\rho^+}^\beta - iJ(\hat{s}) \epsilon_\mu^* + iK(\hat{s}) \\ &\times (\epsilon^* \cdot \hat{p}_B) \hat{p}_\mu + iL(\hat{s}) (\epsilon^* \cdot \hat{p}_B) \hat{q}_\mu, \end{aligned} \quad (41)$$

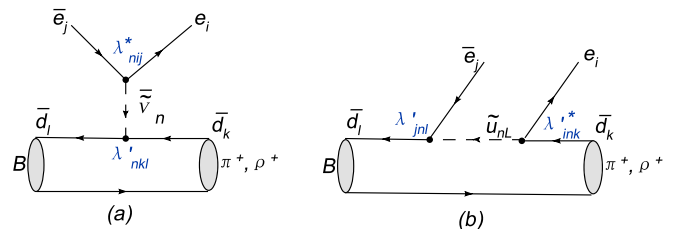


FIG. 1 (color online). The RPV contributions to  $B_u^+ \rightarrow \pi^+ (\rho^+) \ell^+ \ell^-$  due to the sneutrino and squark exchange.

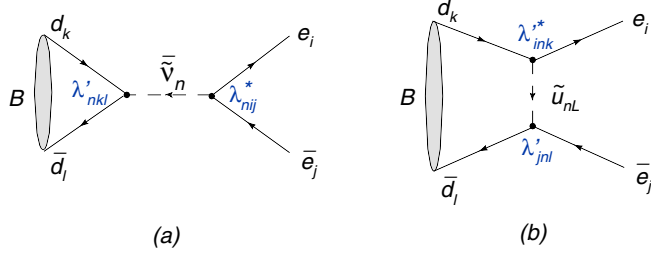


FIG. 2 (color online). The RPV contributions to  $B_d^0 \rightarrow \ell^+ \ell^-$  due to the sneutrino and squark exchange.

$$\Phi_{\bar{\nu}} = \sum_i \frac{\lambda_{ijk} \lambda_{i31}^*}{4m_{\bar{\nu}_{iL}}^2} \left[ -\frac{i}{2} \frac{A_0^{B_u^+ \rightarrow \rho^+}(\hat{s})}{\bar{m}_b + \bar{m}_d} \lambda^{1/2} m_B^2 \right], \quad (42)$$

$$\Phi'_{\bar{\nu}} = \sum_i \frac{\lambda_{ikj}^* \lambda'_{i13}}{4m_{\bar{\nu}_{iL}}^2} \left[ \frac{i}{2} \frac{A_0^{B_u^+ \rightarrow \rho^+}(\hat{s})}{\bar{m}_b + \bar{m}_d} \lambda^{1/2} m_B^2 \right], \quad (43)$$

and the auxiliary functions above are found to be

$$I(\hat{s}) = -\sum_i \frac{\lambda'_{ji3} \lambda_{ki1}^*}{8m_{\bar{\nu}_{iL}}^2} \left[ \frac{2V^{B_u^+ \rightarrow \rho^+}(\hat{s})}{m_B + m_{\rho^+}} m_B^2 \right], \quad (44)$$

$$J(\hat{s}) = \sum_i \frac{\lambda'_{ji3} \lambda_{ki1}^*}{8m_{\bar{\nu}_{iL}}^2} [(m_B + m_{\rho^+}) A_1^{B_u^+ \rightarrow \rho^+}(\hat{s})], \quad (45)$$

$$K(\hat{s}) = -\sum_i \frac{\lambda'_{ji3} \lambda_{ki1}^*}{8m_{\bar{\nu}_{iL}}^2} \left[ \frac{A_2^{B_u^+ \rightarrow \rho^+}(\hat{s})}{m_B + m_{\rho^+}} m_B^2 \right], \quad (46)$$

$$L(\hat{s}) = -\sum_i \frac{\lambda'_{ji3} \lambda_{ki1}^*}{8m_{\bar{\nu}_{iL}}^2} \left[ \frac{2m_{\rho^+}}{\hat{s}} (A_3^{B_u^+ \rightarrow \rho^+}(\hat{s}) - A_0^{B_u^+ \rightarrow \rho^+}(\hat{s})) \right]. \quad (47)$$

For the pure leptonic decays  $B_d^0 \rightarrow \ell^+ \ell^-$ , the RPV amplitude is

$$\begin{aligned} \mathcal{M}^{\#p}(B_d \rightarrow \ell^+ \ell^-) &= \Omega_{\bar{u}}(\bar{\ell}_k \not{p}_B(1 - \gamma_5)\ell_j) \\ &\quad + \Omega_{\bar{\nu}}(\bar{\ell}_k(1 - \gamma_5)\ell_j) \\ &\quad + \Omega'_{\bar{\nu}}(\bar{\ell}_k(1 + \gamma_5)\ell_j), \end{aligned} \quad (48)$$

where

$$\begin{aligned} \Omega_{\bar{u}} &= if_{B_d} \sum_i \frac{\lambda'_{ji3} \lambda_{ki1}^*}{8m_{\bar{\nu}_{iL}}^2}, & \Omega_{\bar{\nu}} &= -if_{B_d} \mu_{B_d} \sum_i \frac{\lambda_{ijk} \lambda_{i31}^*}{4m_{\bar{\nu}_{iL}}^2}, \\ \Omega'_{\bar{\nu}} &= if_{B_d} \mu_{B_d} \sum_i \frac{\lambda_{ikj}^* \lambda'_{i13}}{4m_{\bar{\nu}_{iL}}^2}, \end{aligned} \quad (49)$$

$$\text{and } \mu_{B_d} \equiv \frac{m_{B_d}^2}{\bar{m}_b + \bar{m}_d}.$$

Generally, the RPV couplings can be complex and their phase may induce new contributions, so we write them as

$$\begin{aligned} \lambda_{ijk} \lambda_{lmn}^* &= |\lambda_{ijk} \lambda_{lmn}^*| e^{i\phi_{\#p}}, \\ \lambda_{ijk}^* \lambda_{lmn} &= |\lambda_{ijk} \lambda_{lmn}^*| e^{-i\phi_{\#p}}, \end{aligned} \quad (50)$$

and  $\phi_{\#p} \in [-\pi, \pi]$  is the RPV weak phase.

### C. The branching ratios with RPV contributions

Using the formulas presented above, we get the following results for the double differential decay branching ratios for the decays  $B_u^+ \rightarrow M^+ \ell^+ \ell^-$  ( $M^+ = \pi^+$  or  $\rho^+$ ),

$$\frac{d^2 \mathcal{B}^{M^+}}{d\hat{s} d\hat{u}} = \frac{d^2 \mathcal{B}_{\text{SM}}^{M^+}}{d\hat{s} d\hat{u}} + \frac{d^2 \mathcal{B}_{\bar{u}}^{M^+}}{d\hat{s} d\hat{u}} + \frac{d^2 \mathcal{B}_{\bar{\nu}}^{M^+}}{d\hat{s} d\hat{u}} + \frac{d^2 \mathcal{B}'_{\bar{\nu}}^{M^+}}{d\hat{s} d\hat{u}}. \quad (51)$$

Since it is always assumed in the literature for numerical display that only one sfermion contributes at one time, we have neglected the interferences between different RPV coupling products, but kept their interferences with the SM amplitude, as shown in the following equations.

For the  $B_u^+ \rightarrow \pi^+ \ell^+ \ell^-$  decay,

$$\begin{aligned} \frac{d^2 \mathcal{B}_{\bar{u}}^{\pi^+}}{d\hat{s} d\hat{u}} &= \tau_B \frac{m_B^4}{2^7 \pi^3} \{ \text{Re}(WA'Y_{\bar{u}}^*) (\lambda - \hat{u}^2) + \text{Re}(WC'Y_{\bar{u}}^*) \\ &\quad \times [ -(\lambda - \hat{u}^2) - 4\hat{m}_\ell^2 (2 + 2\hat{m}_{\pi^+}^2 - \hat{s}) ] \\ &\quad + \text{Re}(WD'Y_{\bar{u}}^*) [ -4\hat{m}_\ell^2 (1 - \hat{m}_{\pi^+}^2) ] \\ &\quad + |Y_{\bar{u}}|^2 m_B [\lambda - \hat{u}^2 + 2\hat{m}_\ell^2 (2 + 2\hat{m}_{\pi^+}^2 - \hat{s})] \}, \end{aligned} \quad (52)$$

$$\begin{aligned} \frac{d^2 \mathcal{B}_{\bar{\nu}}^{\pi^+}}{d\hat{s} d\hat{u}} &= \tau_B \frac{m_B^3}{2^7 \pi^3} \{ \text{Re}(WA'Y_{\bar{\nu}}^*) (2\hat{m}_\ell \hat{u}) + \text{Re}(WC'Y_{\bar{\nu}}^*) \\ &\quad \times (1 - \hat{m}_{\pi^+}^2) (-2\hat{m}_\ell) + \text{Re}(WD'Y_{\bar{\nu}}^*) (-2\hat{m}_\ell \hat{s}) \\ &\quad + |Y_{\bar{\nu}}|^2 (\hat{s} - 2\hat{m}_\ell^2) \}, \end{aligned} \quad (53)$$

$$\begin{aligned} \frac{d^2 \mathcal{B}'_{\bar{\nu}}^{\pi^+}}{d\hat{s} d\hat{u}} &= \tau_B \frac{m_B^3}{2^7 \pi^3} \{ \text{Re}(WA'Y_{\bar{\nu}}^*) (2\hat{m}_\ell \hat{u}) + \text{Re}(WC'Y_{\bar{\nu}}^*) \\ &\quad \times (1 - \hat{m}_{\pi^+}^2) (2\hat{m}_\ell) + \text{Re}(WD'Y_{\bar{\nu}}^*) (2\hat{m}_\ell \hat{s}) \\ &\quad + |Y_{\bar{\nu}}'|^2 (\hat{s} - 2\hat{m}_\ell^2) \}, \end{aligned} \quad (54)$$

and  $W = -\frac{G_F \alpha_e}{2\sqrt{2}\pi} V_{ib}^* V_{id} m_B$ .

For the  $B_u^+ \rightarrow \rho^+ \ell^+ \ell^-$  decay,

$$\begin{aligned}
\frac{d^2 \mathcal{B}_u^{\rho^+}}{d\hat{s}d\hat{u}} = & \tau_B \frac{m_B^3}{2^9 \pi^3} \left\{ \text{Re}(WAI^*)[\hat{s}(\lambda + \hat{u}^2) + 4\hat{m}_\ell^2 \lambda] - \text{Re}(WEI^*)[\hat{s}(\lambda + \hat{u}^2) - 4\hat{m}_\ell^2 \lambda] + |I|^2[\hat{s}(\lambda + \hat{u}^2)] \right. \\
& + 4\hat{s}\hat{u}[\text{Re}(WAJ^*) + \text{Re}(WBI^*) - \text{Re}(WEJ^*) - \text{Re}(WFI^*) + 2\text{Re}(IJ^*)] \\
& + \frac{1}{\hat{m}_{\rho^+}^2} [\text{Re}(WBJ^*)(\lambda - \hat{u}^2 + 8\hat{m}_{\rho^+}^2(\hat{s} + 2m_\ell^2)) - \text{Re}(WFJ^*)(\lambda - \hat{u}^2 + 8\hat{m}_{\rho^+}^2(\hat{s} - 4m_\ell^2)) \\
& + |J|^2(\lambda - \hat{u}^2 + 8\hat{m}_{\rho^+}^2(\hat{s} - \hat{m}_\ell^2)) - \text{Re}(WBK^*)(\lambda - \hat{u}^2)(1 - \hat{m}_{\rho^+}^2 - \hat{s}) + \text{Re}(WFK^*)((\lambda - \hat{u}^2)(1 - \hat{m}_{\rho^+}^2 - \hat{s}) \\
& + 4\hat{m}_\ell^2 \lambda) - 2\text{Re}(JK^*)((\lambda - \hat{u}^2)(1 - \hat{m}_{\rho^+}^2 - \hat{s}) + 2\hat{m}_\ell^2 \lambda)] + \frac{\lambda}{\hat{m}_{\rho^+}^2} [\text{Re}(WCK^*)(\lambda - \hat{u}^2) \\
& - \text{Re}(W GK^*)(\lambda - \hat{u}^2 + 4\hat{m}_\ell^2(2 + 2\hat{m}_{\rho^+}^2 - \hat{s})) + |K|^2(\lambda - \hat{u}^2 + 2\hat{m}_\ell^2(2 + 2\hat{m}_{\rho^+}^2 - \hat{s}))] \\
& \left. + \frac{4\hat{m}_\ell^2}{\hat{m}_{\rho^+}^2} \lambda [-\text{Re}(WHL^*)\hat{s} + |L|^2\hat{s}/2 + \text{Re}(WFL^*) - \text{Re}(JL^*) - \text{Re}(WGL^*)(1 - \hat{m}_{\rho^+}^2) + \text{Re}(KL^*)(1 - \hat{m}_{\rho^+}^2)] \right\}, \tag{55}
\end{aligned}$$

$$\begin{aligned}
\frac{d^2 \mathcal{B}_\nu^{\rho^+}}{d\hat{s}d\hat{u}} = & \tau_B \frac{m_B^3}{2^7 \pi^3} \left\{ -\frac{\hat{m}_\ell^2}{\hat{m}_{\rho^+}^2} [\text{Im}(WB\Phi_\nu^*) \right. \\
& \cdot (\lambda^{-1/2}\hat{u}(1 - \hat{m}_{\rho^+}^2 - \hat{s})) + \text{Im}(WC\Phi_\nu^*)\lambda^{1/2}\hat{u} \\
& + \text{Im}(WF\Phi_\nu^*)\lambda^{1/2} - \text{Im}(WG\Phi_\nu^*)\lambda^{1/2}(1 - \hat{m}_{\rho^+}^2)] \\
& \left. + |\Phi_\nu'|^2(\hat{s} - 2\hat{m}_\ell^2) \right\}, \tag{56}
\end{aligned}$$

$$\begin{aligned}
\frac{d^2 \mathcal{B}'_\nu{}^{\rho^+}}{d\hat{s}d\hat{u}} = & \tau_B \frac{m_B^3}{2^7 \pi^3} \left\{ -\frac{\hat{m}_\ell^2}{\hat{m}_{\rho^+}^2} [\text{Im}(WB\Phi_\nu^{*\prime}) \right. \\
& \cdot (\lambda^{-1/2}\hat{u}(1 - \hat{m}_{\rho^+}^2 - \hat{s})) + \text{Im}(WC\Phi_\nu^{*\prime})\lambda^{1/2}\hat{u} \\
& - \text{Im}(WF\Phi_\nu^{*\prime})\lambda^{1/2} + \text{Im}(WG\Phi_\nu^{*\prime})\lambda^{1/2}(1 - \hat{m}_{\rho^+}^2)] \\
& \left. + |\Phi_\nu'|^2(\hat{s} - 2\hat{m}_\ell^2) \right\}. \tag{57}
\end{aligned}$$

The normalized forward-backward asymmetries is defined by

$$\begin{aligned}
\mathcal{A}_{\text{FB}}(B \rightarrow M\ell^+\ell^-) & \\
= & \int d\hat{s} \frac{\int_{-1}^{+1} \frac{d^2 \mathcal{B}(B \rightarrow M\ell^+\ell^-)}{d\hat{s}d\cos\theta} \text{sign}(\cos\theta) d\cos\theta}{\int_{-1}^{+1} \frac{d^2 \mathcal{B}(B \rightarrow M\ell^+\ell^-)}{d\hat{s}d\cos\theta} d\cos\theta}. \tag{58}
\end{aligned}$$

Since there is no term containing  $\hat{u}$  with an odd power as shown by Eq. (30), the  $\mathcal{A}_{\text{FB}}$  is zero for  $B_u^+ \rightarrow \pi^+\ell^+\ell^-$  decays in the SM. The RPV effect via squark exchange on  $\mathcal{A}_{\text{FB}}(B_u^+ \rightarrow \pi^+\ell^+\ell^-)$  also vanishes for the same reason as shown by Eq. (52), while the sneutrino exchange contributions to  $\mathcal{A}_{\text{FB}}$ , as shown by Eqs. (53) and (54), are proportional to  $m_\ell$ , which are tiny for  $\ell = e, \mu$ .

The total decay branching ratios of the pure leptonic  $B_d^0$  decays are given by

$$\begin{aligned}
\mathcal{B}(B_d \rightarrow \ell^+\ell^-) = & \mathcal{B}^{\text{SM}}(B_d \rightarrow \ell^+\ell^-) \left\{ 1 + \frac{1}{|K_{\text{SM}}|^2} \right. \\
& \times [2\text{Re}(K_{\text{SM}}\Omega_u^*) + |\Omega_u^-|^2] \\
& + \frac{1}{|K_{\text{SM}}|^2} \left[ \text{Re}(K_{\text{SM}}\Omega_\nu^*) \frac{1}{m_\ell} \right. \\
& \left. + |\Omega_\nu|^2 \left( \frac{1}{2m_\ell^2} - \frac{1}{m_{B_d}^2} \right) \right] \\
& + \frac{1}{|K_{\text{SM}}|^2} \left[ -\text{Re}(K_{\text{SM}}\Omega_\nu^{*\prime}) \frac{1}{m_\ell} \right. \\
& \left. + |\Omega_\nu^{\prime}|^2 \left( \frac{1}{2m_\ell^2} - \frac{1}{m_{B_d}^2} \right) \right] \right\}, \tag{59}
\end{aligned}$$

with

$$K_{\text{SM}} = -\frac{G_F}{\sqrt{2}} \frac{\alpha_e}{2\pi \sin 2\theta_W} V_{td} V_{tb}^* Y(x_t) (if_{B_d}). \tag{60}$$

From Eq. (59), we can see that  $\mathcal{B}(B_d^0 \rightarrow \ell^+\ell^-)$  could be enhanced very much by the  $s$ -channel RPV sneutrino exchange, but not so much by the  $t$ -channel squark exchange.

### III. NUMERICAL RESULTS AND ANALYSES

With the formulas presented in previous section, we are ready to perform our numerical analysis. First, we will specify the input parameters. Then we will use the latest up-limits of  $\mathcal{B}(B_u^+ \rightarrow \pi^+\ell^+\ell^-)$  and  $\mathcal{B}(B_d^0 \rightarrow \ell^+\ell^-)$  to get the constraints on the relevant RPV couplings. Finally, we will show the distributions of the branching ratios and the forward-backward asymmetries of these decays in the constrained RPV parameter space.

In the Wolfenstein parametrization of the CKM matrix elements, one has

TABLE I. Fit for form factors involving the  $B \rightarrow \pi(\rho)$  transitions valid for general  $q^2$  [27].

$F(\hat{s})$	$F(0)$	$\Delta_{\text{tot}}$	$r_1$	$m_R^2$	$r_2$	$m_{\text{fit}}^2$	fit Eq.
$f_+^{B \rightarrow \pi}$	0.258	0.031	0.744	$5.32^2$	-0.486	40.73	(63)
$f_T^{B \rightarrow \pi}$	0.253	0.028	1.387	$5.32^2$	-1.134	32.22	(63)
$f_0^{B \rightarrow \pi}$	0.258	0.031			0.258	33.81	(65)
$V^{B \rightarrow \rho}$	0.323	0.030	1.045	$5.32^2$	-0.721	38.34	(63)
$A_0^{B \rightarrow \rho}$	0.303	0.029	1.527	$5.28^2$	-1.220	33.36	(63)
$A_1^{B \rightarrow \rho}$	0.242	0.023			0.240	37.51	(65)
$A_2^{B \rightarrow \rho}$	0.221	0.023	0.009		0.212	40.82	(64)
$T_1^{B \rightarrow \rho}$	0.267	0.023	0.897	$5.32^2$	-0.629	38.04	(63)
$T_2^{B \rightarrow \rho}$	0.267	0.023			0.267	38.59	(65)
$\tilde{T}_3^{B \rightarrow \rho}$	0.267	0.024	0.022		0.246	40.88	(64)

$$\lambda_u^* = \frac{V_{ub}^* V_{ud}}{V_{tb}^* V_{td}} = \frac{\bar{\rho} + i\bar{\eta}}{1 - \bar{\rho} - i\bar{\eta}} + O(\lambda^5). \quad (61)$$

The parameters  $\lambda$ ,  $\bar{\rho}$  and  $\bar{\eta}$  have been updated by CKMfitter Group [39], which read

$$\lambda = 0.22568^{+0.00084}_{-0.00079}, \quad \bar{\rho} = 0.213^{+0.014}_{-0.024}, \quad (62)$$

$$\bar{\eta} = 0.348^{+0.012}_{-0.021}.$$

In our numerical analysis, we have used  $|V_{td} V_{tb}^*| = |V_{td}| = (8.27^{+0.21}_{-0.49}) \times 10^{-3}$  [39].

For the semileptonic decays  $B_u^+ \rightarrow \pi^+ \ell^+ \ell^-$  and  $B_u^+ \rightarrow \rho^+ \ell^+ \ell^-$ , we will use the form factors of light-cone QCD sum rules (LCSRs) results [27], which are renewed recently with radiative corrections to the leading twist

wave functions and  $SU(3)$  breaking effects. For the  $q^2$  dependence of the form factors, they are parametrized in terms of simple formulas with two or three parameters. The form factors  $V, A_0, T_1, f_+$ , and  $f_T$  are parametrized by [27]

$$F(\hat{s}) = \frac{r_1}{1 - \hat{s}/\hat{m}_R^2} + \frac{r_2}{1 - \hat{s}/\hat{m}_{\text{fit}}^2}. \quad (63)$$

For the form factors  $A_2$  and  $\tilde{T}_3$ , it is more appropriate to expand them to the second order around the pole [27]

$$F(\hat{s}) = \frac{r_1}{1 - \hat{s}/\hat{m}_{\text{fit}}^2} + \frac{r_2}{(1 - \hat{s}/\hat{m}_{\text{fit}}^2)^2}. \quad (64)$$

The fit formula for  $A_1, T_2$  and  $f_0$  is

$$F(\hat{s}) = \frac{r_2}{1 - \hat{s}/\hat{m}_{\text{fit}}^2}. \quad (65)$$

The form factor  $T_3$  can be obtained with  $T_3(\hat{s}) = \frac{1-\hat{m}_\rho}{\hat{s}} \times [\tilde{T}_3(\hat{s}) - T_2(\hat{s})]$ . The values of all the corresponding parameters for these form factors are listed in Table I, the uncertainties induced by  $F(0)$  [27] are also considered in the following numerical data analyses.

The values of other input parameters used in the numerical calculation and the experimental upper-limits are given, respectively, in Tables II and III. In the numerical calculations through the paper, we will take into account of the  $1\sigma$  uncertainties of the parameters with relative large error bars.

With these inputs, we get the SM predictions in Table III, where the  $1\sigma$  error bar are obtained simply with a Gaussian distribution treatment of the outputs caused by the uncertainties of input parameters. To get

TABLE II. Default values of the input parameters and the  $\pm 1\sigma$  error bars of the sensitive parameters used in our numerical calculations in addition to the ones discussed in text.

$m_{B_d} = 5.279$ GeV, $m_{B_u} = 5.279$ GeV, $m_W = 80.425$ GeV,	
$m_{\pi^+} = 0.140$ GeV, $m_{\pi^0} = 0.135$ GeV, $m_\rho = 0.776$ GeV,	
$\bar{m}_b(\bar{m}_b) = (4.20 \pm 0.07)$ GeV,	
$\bar{m}_u(2 \text{ GeV}) = 0.0015 \sim 0.003$ GeV, $\bar{m}_d(2 \text{ GeV}) = 0.003 \sim 0.007$ GeV,	
$m_e = 0.511 \times 10^{-3}$ GeV, $m_\mu = 0.106$ GeV, $m_{t,\text{pole}} = 174.2 \pm 3.3$ GeV.	[28]
$\tau_{B_d} = 1.530$ ps, $\tau_{B_u} = 1.638$ ps.	[28]
$\sin^2 \theta_W = 0.22306$ , $\alpha_e = 1/137$ .	[28]
$f_{B_d} = 0.216^{+0.009}_{-0.019}$ GeV.	[40]

TABLE III. The SM predictions and experimental data of branching ratios for the upper limits for  $B_d^0 \rightarrow \ell^+ \ell^-$  and  $B_u^+ \rightarrow \pi^+ \ell^+ \ell^-$  [15,17,41].

	SM prediction value	Experimental data
$\mathcal{B}(B_u^+ \rightarrow \pi^+ \mu^+ \mu^-)$	$(2.03 \pm 0.23) \times 10^{-8}$	$< 2.8 \times 10^{-7}$ (90% C.L.) [15]
$\mathcal{B}(B_u^+ \rightarrow \pi^+ e^+ e^-)$	$(2.03 \pm 0.23) \times 10^{-8}$	$< 1.8 \times 10^{-7}$ (90% C.L.) [15]
$\mathcal{B}(B_u^+ \rightarrow \rho^+ \mu^+ \mu^-)$	$(4.33 \pm 1.14) \times 10^{-8}$	
$\mathcal{B}(B_u^+ \rightarrow \rho^+ e^+ e^-)$	$(5.26 \pm 1.37) \times 10^{-8}$	
$\mathcal{B}(B_d \rightarrow \mu^+ \mu^-)$	$(1.33 \pm 0.12) \times 10^{-10}$	$< 1.5 \times 10^{-8}$ (90% C.L.) [17]
$\mathcal{B}(B_d \rightarrow e^+ e^-)$	$(3.11 \pm 0.27) \times 10^{-15}$	$< 6.1 \times 10^{-8}$ (90% C.L.) [41]

conservative (realistic) constrains on RPV effects, we would take the whole possible regions of the distributions due to the variances of input parameters as the SM predictions, which are listed in Table V. We find our result  $\mathcal{B}(B_u^+ \rightarrow \pi^+ \ell^+ \ell^-) = (2.03 \pm 0.23) \times 10^{-8}$  is smaller than the value  $3.27 \times 10^{-8}$  in Ref. [19]. The difference is mainly due to the updated values for form factors and CKM parameters.

As in the literature, we assume that only one sfermion contributes at one time with a mass of 100 GeV. For other values of the sfermion masses, the bounds on the couplings in this paper can be easily obtained by scaling them by factor  $\tilde{f}^2 \equiv (\frac{m_{\tilde{f}}}{100 \text{ GeV}})^2$ . In Table III, the relevant experimental upper limits [15,17,41] are listed for comparison. We can see that the experimental upper limits of  $\mathcal{B}(B_u^+ \rightarrow \pi^+ \ell^+ \ell^-)$  are just one order above the SM expectations, which will constrain RPV SUSY parameter space significantly. Although the present limit of  $\mathcal{B}(B_d^0 \rightarrow \mu^+ \mu^-)$  are 2 orders of magnitude higher than the SM prediction, the upper-limit will also yield strong bounds since the decay  $B_d^0 \rightarrow \mu^+ \mu^-$  is very sensitive to new pseudoscalar interactions beyond the SM.

Now we turn to the RPV effects. The decays to  $B_u^+ \rightarrow \rho^+ \ell^+ \ell^-$ ,  $B_u^+ \rightarrow \pi^+ \ell^+ \ell^-$ , and  $B_d^0 \rightarrow \ell^+ \ell^-$  involve the same set of the six RPV coupling products. Combining the upper-limits of  $\mathcal{B}(B_u^+ \rightarrow \pi^+ \ell^+ \ell^-)$  [15] and  $\mathcal{B}(B_d^0 \rightarrow \ell^+ \ell^-)$  [17,28] listed in Table III, we get constraints on the six RPV coupling products. Subject to the constraints, the random variations of the parameters as discussed previously lead to the scatter plots displayed in Fig. 3. From the figure, we can see that the RPV constraints on  $\lambda'_{213} \lambda_{2i1}^*$  and  $\lambda'_{1i3} \lambda_{i1}^*$  are sensitive to their RPV weak phases, which implies significant interferences between the squark contributions and the SM ones. As depicted by Figs. 1 and 2, the squark contribution amplitudes are of  $\bar{b}(V+A)d\bar{\ell}(V-A)$  current structure after Fierz transformations, which are similar to the SM amplitudes. For the constraints on  $\lambda' \lambda^*$  of sneutrinos are insensitive to their phase  $\phi_{\tilde{\nu}_p}$ . We summarize all the constraints in Table IV, where the recent updated bounds [42] are listed for comparison. It is shown that our bounds are more restricted than the previous ones. We note that the strong constraints on  $\lambda'_{1i3} \lambda_{i1}^*$  and  $\lambda'_{2i3} \lambda_{2i1}^*$  are mainly due to the upper-limits of  $\mathcal{B}(B^+ \rightarrow \pi^+ \ell^+ \ell^-)$ , which are just one order higher than the SM expectations,

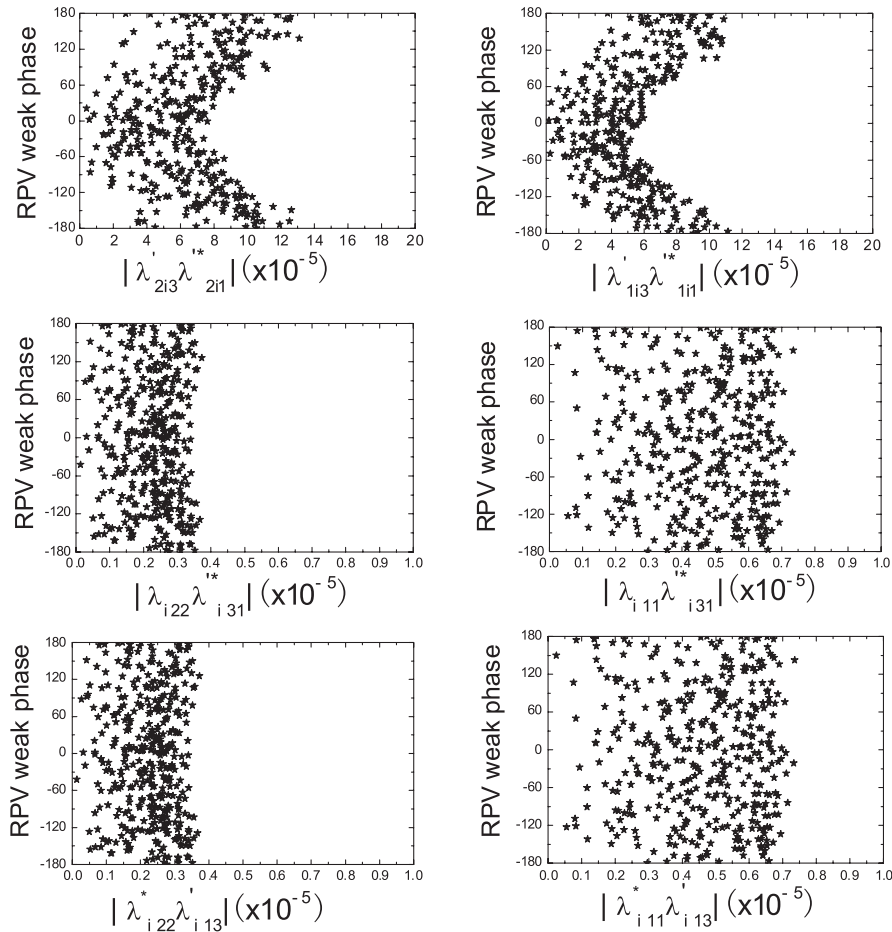


FIG. 3. The allowed parameter spaces for the relevant RPV couplings constrained by the measurements listed in Table III, and the RPV weak phase is given in degree.



TABLE IV. Bounds for the relevant RPV couplings products by  $B_u^+ \rightarrow \pi^+ \ell^+ \ell^-$  and  $B_d^0 \rightarrow \ell^+ \ell^-$  decays for 100 GeV sfermions. For comparison, we list previous bounds which are also obtained with the sfermion masses of 100 GeV.

Couplings	Bounds [Processes]	Previous bounds [Processes] [42]
$ \lambda'_{i13} \lambda_{i11}^* $	$\leq 1.1 \times 10^{-4} \frac{[B_d \rightarrow e^+ e^-]}{[B_u^+ \rightarrow \pi^+ e^+ e^-]}$	$\leq 2.6 \times 10^{-2} [B_d \rightarrow e^+ e^-]$
$ \lambda_{i11} \lambda_{i31}^* $	$\leq 7.4 \times 10^{-6} \frac{[B_d \rightarrow e^+ e^-]}{[B_u^+ \rightarrow \pi^+ e^+ e^-]}$	$\leq 4.1 \times 10^{-5} [B_d \rightarrow e^+ e^-]$
$ \lambda_{i11}^* \lambda'_{i13} $	$\leq 7.4 \times 10^{-6} \frac{[B_d \rightarrow e^+ e^-]}{[B_u^+ \rightarrow \pi^+ e^+ e^-]}$	$\leq 4.1 \times 10^{-5} [B_d \rightarrow e^+ e^-]$
$ \lambda'_{2i3} \lambda_{2i1}^* $	$\leq 1.3 \times 10^{-4} \frac{[B_d \rightarrow \mu^+ \mu^-]}{[B_u^+ \rightarrow \pi^+ \mu^+ \mu^-]}$	$\leq 5.4 \times 10^{-4} [B_d \rightarrow \mu^+ \mu^-]$
$ \lambda_{i22} \lambda_{i31}^* $	$\leq 3.7 \times 10^{-6} \frac{[B_d \rightarrow \mu^+ \mu^-]}{[B_u^+ \rightarrow \pi^+ \mu^+ \mu^-]}$	$\leq 6.2 \times 10^{-6} [B_d \rightarrow \mu^+ \mu^-]$
$ \lambda_{i22}^* \lambda'_{i13} $	$\leq 3.7 \times 10^{-6} \frac{[B_d \rightarrow \mu^+ \mu^-]}{[B_u^+ \rightarrow \pi^+ \mu^+ \mu^-]}$	$\leq 6.2 \times 10^{-6} [B_d \rightarrow \mu^+ \mu^-]$

and the constraints on other four RPV coupling products from the sneutrino exchange are mainly due to the upper-limits of  $\mathcal{B}(B_d^0 \rightarrow \ell^+ \ell^-)$ .

Using the constrained parameter spaces shown in Table IV and Fig. 3, one can predict the RPV effects on the other quantities which have not been well measured yet in these processes. We perform a scan over the input parameters and the new constrained RPV coupling spaces to get the allowed ranges for  $\mathcal{B}(B_u^+ \rightarrow \rho^+ \ell^+ \ell^-)$ ,  $\mathcal{B}(B_u^+ \rightarrow \pi^+ \ell^+ \ell^-)$ ,  $\mathcal{B}(B_d^0 \rightarrow \ell^+ \ell^-)$ ,  $\mathcal{A}_{\text{FB}}(B_u^+ \rightarrow \pi^+ \ell^+ \ell^-)$ , and  $\mathcal{A}_{\text{FB}}(B_u^+ \rightarrow \rho^+ \ell^+ \ell^-)$  with the different RPV couplings products. The numerical results are summarized in Table V.

For Table V, we have the following remarks.

- (i) As shown by Fig. 2(b), the contributions of  $\lambda'_{i13} \lambda_{i11}^*$  and  $\lambda'_{2i3} \lambda_{2i1}^*$  to  $\mathcal{B}(B_d^0 \rightarrow e^+ e^-)$  and  $\mathcal{B}(B_d^0 \rightarrow \mu^+ \mu^-)$ , respectively, arise from  $t$ -channel squark exchange. After Fierz transformation, the effective Hamiltonian due to the  $t$ -channel squark exchange is proportional to  $\bar{b} \gamma^\mu P_R d \bar{\ell} \gamma_\mu P_L \ell$ , which contributions to  $\mathcal{B}(B_d^0 \rightarrow \ell^+ \ell^-)$  are suppressed by  $m_\ell^2/m_B^2$  due to helicity suppression. Therefore,  $\mathcal{B}(B_d^0 \rightarrow e^+ e^-, \mu^+ \mu^-)$  will not be enhanced so much by the  $t$ -channel squark exchanging RPV contributions. In other words, the bounds on these two RPV cou-

pling products are due to the upper-limits of  $\mathcal{B}(B_u^+ \rightarrow \pi^+ \ell^+ \ell^-)$ . With the bounds, the RPV squark exchanges could enhance  $\mathcal{B}(B_d^0 \rightarrow e^+ e^-)$  and  $\mathcal{B}(B_d^0 \rightarrow \mu^+ \mu^-)$ , to the utmost, to  $6.7 \times 10^{-14}$  and  $3.9 \times 10^{-9}$ , respectively. However, the effective Hamiltonian of  $s$ -channel sneutrino exchange would be  $\bar{b}(1 \pm \gamma_5) d \bar{\ell}(1 \mp \gamma_5) \ell$ , whose contributions are not suppressed by  $m_\ell^2/m_B^2$ . Therefore, both  $\mathcal{B}(B_d^0 \rightarrow e^+ e^-)$  and  $\mathcal{B}(B_d^0 \rightarrow \mu^+ \mu^-)$  could be enhanced to order of  $10^{-8}$  to saturate their experimental upper limits by  $\lambda_{i11} \lambda_{i31}^*$  and  $\lambda_{i22} \lambda_{i31}^*$ , respectively.

- (ii) At present there is no experimental data for  $B_u^+ \rightarrow \rho^+ \ell^+ \ell^-$  decays. It is interesting to note that  $\mathcal{B}(B_u^+ \rightarrow \rho^+ \ell^+ \ell^-)$  could be enhanced to order of  $10^{-6}$  by the  $t$ -channel squark exchange within the bounds due to the upper-limits of  $\mathcal{B}(B_u^+ \rightarrow \pi^+ \ell^+ \ell^-)$ , however, it is not sensitive to the  $s$ -channel sneutrino exchanges within the constrained parameter space.
- (iii)  $\mathcal{A}_{\text{FB}}(B_u^+ \rightarrow \pi^+ e^+ e^-)$  and  $\mathcal{A}_{\text{FB}}(B_u^+ \rightarrow \pi^+ \mu^+ \mu^-)$  are zero in the SM. The RPV contributions to the asymmetries due to squark exchanging are also zero, while the sneutrino exchanging RPV contributions are also too small to be accessible at the LHC.

TABLE V. The results for  $\mathcal{B}(B_d^0 \rightarrow \ell^+ \ell^-)$ ,  $\mathcal{B}(B_u^+ \rightarrow \rho^+ \ell^+ \ell^-)$ ,  $\mathcal{B}(B_u^+ \rightarrow \pi^+ \ell^+ \ell^-)$ , and  $\mathcal{A}_{\text{FB}}(B_u^+ \rightarrow \pi^+ (\rho^+) \ell^+ \ell^-)$  in the SM and the RPV SUSY. The RPV SUSY predictions are obtained by the allowed regions of the different RPV couplings products. In the RPV couplings,  $g = 1$  and  $2$  for  $\ell = e$  and  $\mu$ , respectively.

	SM value	$\lambda'_{gi3} \lambda_{gi1}^*$	$\lambda_{igg} \lambda_{i31}^*$	$\lambda_{igg}^* \lambda'_{i13}$
$\mathcal{B}(B_d^0 \rightarrow e^+ e^-)$	$[2.2, 3.7] \times 10^{-15}$	$[0.002, 6.7] \times 10^{-14}$	$[0.008, 6.1] \times 10^{-8}$	$[0.008, 6.1] \times 10^{-8}$
$\mathcal{B}(B_u^+ \rightarrow \pi^+ e^+ e^-)$	$[1.4, 2.6] \times 10^{-8}$	$[0.57, 18.0] \times 10^{-8}$	$[1.6, 15.5] \times 10^{-8}$	$[1.7, 13.8] \times 10^{-8}$
$\mathcal{B}(B_u^+ \rightarrow \rho^+ e^+ e^-)$	$[2.8, 9.7] \times 10^{-8}$	$[3.8586.8] \times 10^{-8}$	$[2.9, 10.2] \times 10^{-8}$	$[2.8, 10.2] \times 10^{-8}$
$\mathcal{A}_{\text{FB}}(B_u^+ \rightarrow \pi^+ e^+ e^-)$	0	0	$[-7.2, 6.7] \times 10^{-5}$	$[-7.2, 7.2] \times 10^{-5}$
$\mathcal{A}_{\text{FB}}(B_u^+ \rightarrow \rho^+ e^+ e^-)$	[0.14, 0.23]	[-0.13, 0.82]	[0.14, 0.23]	[0.15, 0.23]
$\mathcal{B}(B_d^0 \rightarrow \mu^+ \mu^-)$	$[0.96, 1.56] \times 10^{-10}$	$[0.01, 38.9] \times 10^{-10}$	$[0.01, 1.5] \times 10^{-8}$	$[0.01, 1.5] \times 10^{-8}$
$\mathcal{B}(B_u^+ \rightarrow \pi^+ \mu^+ \mu^-)$	$[1.4, 2.6] \times 10^{-8}$	$[0.22, 27.92] \times 10^{-8}$	$[1.7, 5.3] \times 10^{-8}$	$[1.6, 5.4] \times 10^{-8}$
$\mathcal{B}(B_u^+ \rightarrow \rho^+ \mu^+ \mu^-)$	$[2.8, 8.4] \times 10^{-8}$	$[3.5780.4] \times 10^{-8}$	$[2.8, 9.1] \times 10^{-8}$	$[2.8, 9.1] \times 10^{-8}$
$\mathcal{A}_{\text{FB}}(B_u^+ \rightarrow \pi^+ \mu^+ \mu^-)$	0	0	$[-1.1, 1.1] \times 10^{-2}$	$[-1.1, 1.1] \times 10^{-2}$
$\mathcal{A}_{\text{FB}}(B_u^+ \rightarrow \rho^+ \mu^+ \mu^-)$	[0.14, 0.23]	[-0.13, 0.46]	[0.14, 0.23]	[0.14, 0.24]

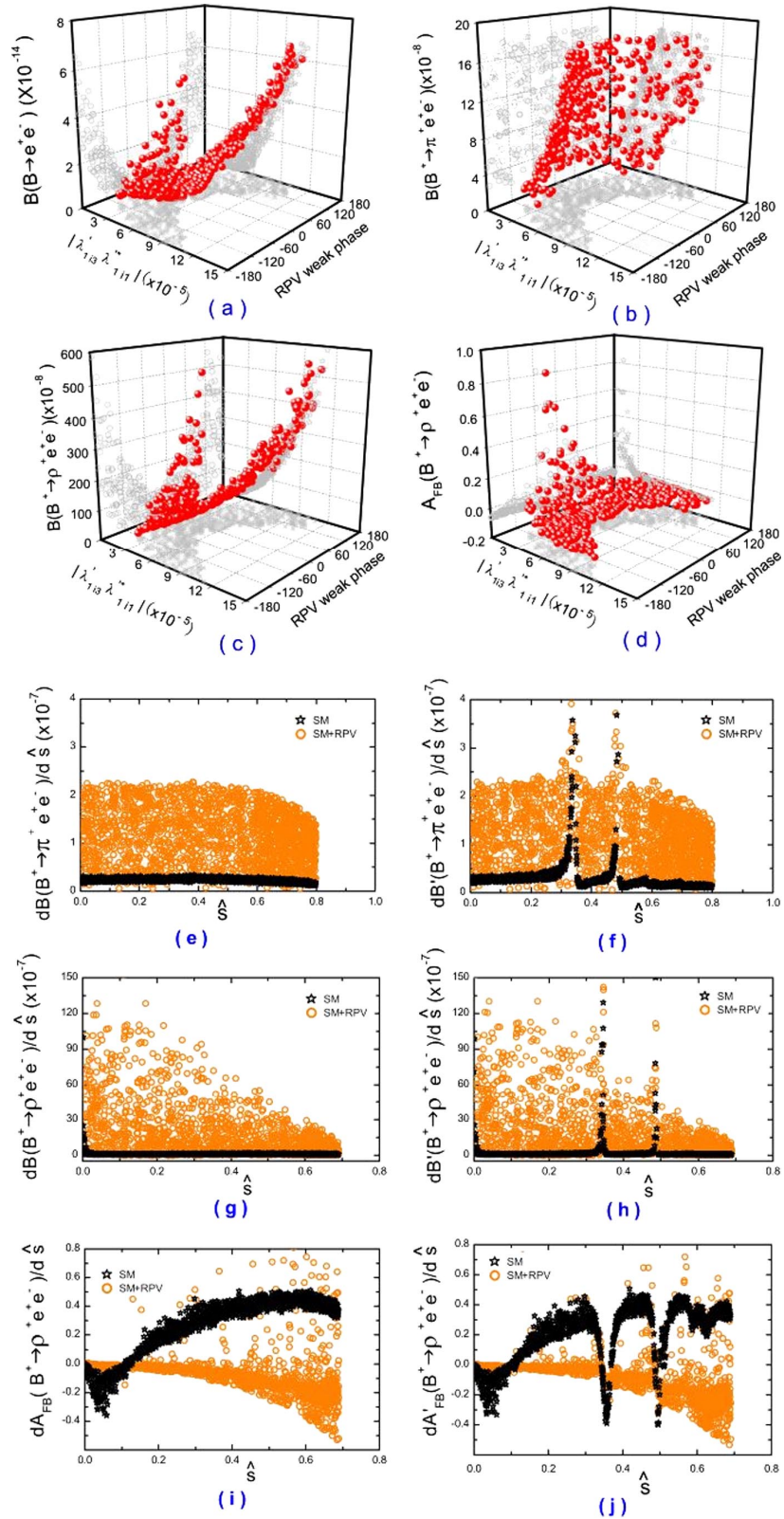


FIG. 4 (color online). The effects of RPV coupling  $\lambda'_{i3}\lambda_{i1}$  due to the squark exchange in  $B_u^+ \rightarrow \pi^+ e^+ e^-$ ,  $B_u^+ \rightarrow \rho^+ e^+ e^-$ , and  $B_d^0 \rightarrow e^+ e^-$  decays. The primed observables are given with  $\psi(nS)$  VMD contributions.

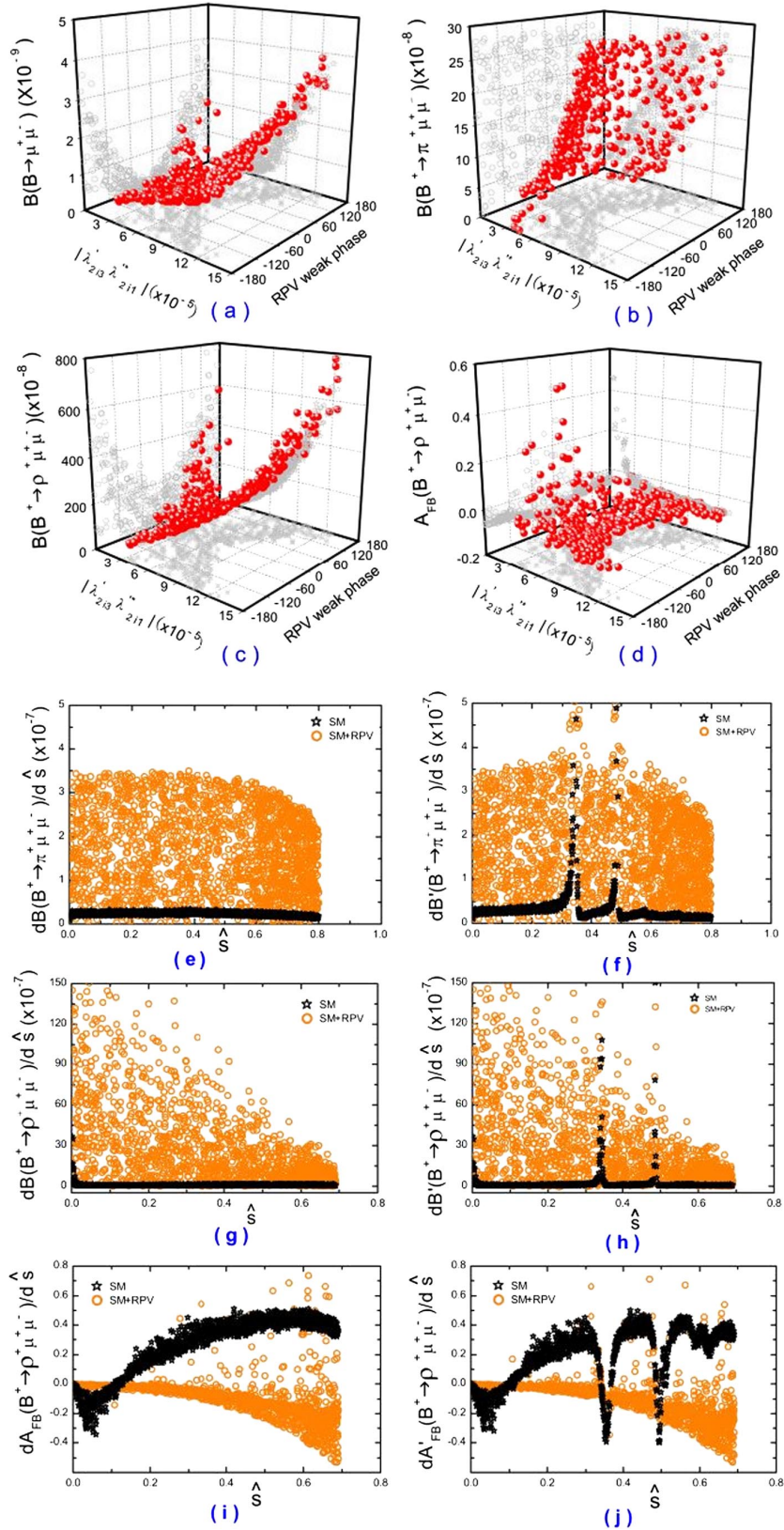


FIG. 5 (color online). The effects of RPV coupling  $\lambda'_{2i3} \lambda_{2i1}^{*/}$  due to the squark exchange in  $B_u^+ \rightarrow \pi^+ \mu^+ \mu^-$ ,  $B_u^+ \rightarrow \rho^+ \mu^+ \mu^-$ , and  $B_d^0 \rightarrow \mu^+ \mu^-$  decays.

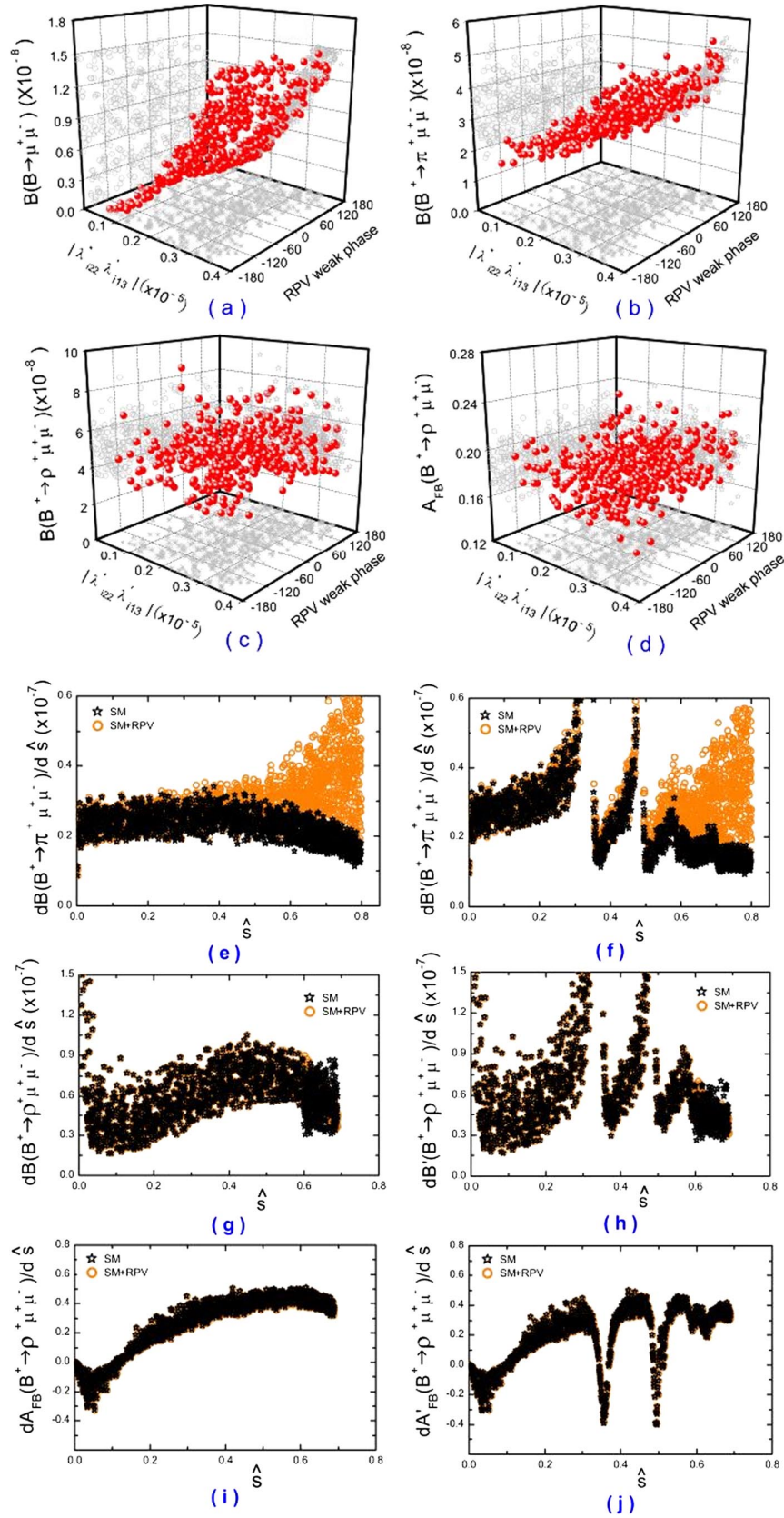


FIG. 6 (color online). The effects of RPV coupling  $\lambda_{i22}^* \lambda_{i13}^l$  due to the sneutrino exchange in  $B_u^+ \rightarrow \pi^+ \mu^+ \mu^-$ ,  $B_u^+ \rightarrow \rho^+ \mu^+ \mu^-$ , and  $B_d^0 \rightarrow \mu^+ \mu^-$  decays.

- (iv) It is found that the squark exchanging RPV contributions have significant impacts on  $\mathcal{A}_{\text{FB}}(B_u^+ \rightarrow \rho^+ e^+ e^-)$  and  $\mathcal{A}_{\text{FB}}(B_u^+ \rightarrow \rho^+ \mu^+ \mu^-)$ . While, the RPV contributions due to the sneutrino exchange affect  $\mathcal{A}_{\text{FB}}(B_u^+ \rightarrow \rho^+ e^+ e^-)$  and  $\mathcal{A}_{\text{FB}}(B_u^+ \rightarrow \rho^+ \mu^+ \mu^-)$  slightly.

For each RPV coupling product, we present the distributions and correlations of branching ratios and forward-backward asymmetries within the constrained parameter space in Fig. 3. Numerical results are shown in Figs. 4–6, where correlations between the physical observable  $\mathcal{B}$ ,  $\mathcal{A}_{\text{FB}}$  and the parameter spaces of the different RPV coupling products by the three-dimensional scatter plots. The dilepton invariant mass distribution and the normalized forward-backward asymmetry are given with vector meson dominance (VMD) contribution excluded in terms of  $d\mathcal{B}/d\hat{s}$  and  $d\mathcal{A}_{\text{FB}}/d\hat{s}$ , and included in  $d\mathcal{B}'/d\hat{s}$  and  $d\mathcal{A}'_{\text{FB}}/d\hat{s}$ , respectively. From Figs. 4–6, one can find the correlations of these physical observable with the RPV coupling products.

Now we turn to discuss plots of Fig. 4 in detail. The three-dimensional scatter plot shows  $\mathcal{A}_{\text{FB}}$  and  $\mathcal{B}$  correlated with  $|\lambda'_{1i3}\lambda_{1i1}^*|$  and its phase  $\phi_{\mathcal{R}_p}$ . We also give projections on three vertical planes, where the  $|\lambda'_{1i3}\lambda_{1i1}^*|-\phi_{\mathcal{R}_p}$  plane displays the constrained regions of  $\lambda'_{1i3}\lambda_{1i1}^*$  as the second plot of Fig. 3. From plots of Fig. 4(a)–4(c), we can find that  $\mathcal{B}(B_d^0 \rightarrow e^+ e^-)$ ,  $\mathcal{B}(B_u^+ \rightarrow \pi^+ e^+ e^-)$  and  $\mathcal{B}(B_u^+ \rightarrow \rho^+ e^+ e^-)$  are increasing with  $|\lambda'_{1i3}\lambda_{1i1}^*|$  on the  $\mathcal{B}-|\lambda'_{1i3}\lambda_{1i1}^*|$  planes, and  $\mathcal{B}(B_u^+ \rightarrow \pi^+ e^+ e^-)$  can be enhanced to its present experimental upper limit. Figure 4(d) shows that  $\mathcal{A}_{\text{FB}}(B_u^+ \rightarrow \rho^+ e^+ e^-)$  is decreasing with  $|\lambda'_{1i3}\lambda_{1i1}^*|$  on the  $\mathcal{A}_{\text{FB}}(B_u^+ \rightarrow \rho^+ e^+ e^-)-|\lambda'_{1i3}\lambda_{1i1}^*|$  plane. It is shown that  $\mathcal{B}(B_d^0 \rightarrow e^+ e^-)$ ,  $\mathcal{B}(B_u^+ \rightarrow \rho^+ e^+ e^-)$  and  $\mathcal{A}_{\text{FB}}(B_u^+ \rightarrow \rho^+ e^+ e^-)$  are sensitive to  $\phi_{\mathcal{R}_p}$  with the first two increasing with  $|\phi_{\mathcal{R}_p}|$  while the last one decreasing, whereas  $\mathcal{B}(B_u^+ \rightarrow \pi^+ e^+ e^-)$  is insensitive to  $\phi_{\mathcal{R}_p}$ . From Figs. 4(e) and 4(f), we can find that the  $\lambda'_{1i3}\lambda_{1i1}^*$  contributions are significantly larger than the SM contributions at the all  $\hat{s}$  regions with theoretical uncertainties included. While for  $d\mathcal{B}(B_u^+ \rightarrow \rho^+ e^+ e^-)/d\hat{s}$ , the RPV effect is significant at the low  $\hat{s}$  region. Especially from Fig. 4(i) and 4(j), we find the RPV contributions to  $d\mathcal{A}'_{\text{FB}}(B_u^+ \rightarrow \rho^+ e^+ e^-)/d\hat{s}$  are quite different from the SM expectations. All the above observations can be extended to Fig. 5, but for squark  $\tilde{u}_{iL}$  contributions to  $B_d^0 \rightarrow \mu^+ \mu^-$ ,  $B_u^+ \rightarrow \pi^+ \mu^+ \mu^-$ , and  $B_u^+ \rightarrow \rho^+ \mu^+ \mu^-$ , instead.

The RPV sneutrino exchange contributions to  $B_u^+ \rightarrow \rho^+ \ell^+ \ell^-$ ,  $B_u^+ \rightarrow \pi^+ \ell^+ \ell^-$ , and  $B_d^0 \rightarrow \ell^+ \ell^-$  are very similar to each other. We would take  $\lambda_{i22}^* \lambda'_{i13}$  contributions as an example, which is shown by Fig. 6. Figures 6(a) and 6(b) show that both  $\mathcal{B}(B_d^0 \rightarrow \mu^+ \mu^-)$  and  $\mathcal{B}(B_u^+ \rightarrow \pi^+ \mu^+ \mu^-)$  are increasing with  $|\lambda_{i22}^* \lambda'_{i13}|$  on the  $\mathcal{B}-|\lambda_{i22}^* \lambda'_{i13}|$  planes, but insensitive to  $\phi_{\mathcal{R}_p}$ , and  $\mathcal{B}(B_d^0 \rightarrow \mu^+ \mu^-)$  can be enhanced to  $\sim 1.5 \times 10^{-8}$  which saturates its present upper

limit. As shown by Figs. 6(c) and 6(d), both  $\mathcal{A}_{\text{FB}}(B_u^+ \rightarrow \rho^+ \mu^+ \mu^-)$  and  $\mathcal{B}(B_u^+ \rightarrow \rho^+ \mu^+ \mu^-)$  are insensitive to the RPV sneutrino contribution. The scatters of points in Figs. 6(c) and 6(d) are due to theoretical uncertainties. The similar situation is also found for the distributions of  $d\mathcal{A}_{\text{FB}}(B_u^+ \rightarrow \rho^+ \mu^+ \mu^-)/d\hat{s}$  and  $d\mathcal{B}(B_u^+ \rightarrow \rho^+ \mu^+ \mu^-)/d\hat{s}$ . From Figs. 6(g)–6(j), one can find that the present theoretical uncertainties in our numerical calculation are still very large, and the RPV sneutrino exchange contributions are indistinguishable from the uncertainties. Figures 6(e) and 6(f) are the distributions of  $d\mathcal{B}^{(l)}(B_u^+ \rightarrow \pi^+ \mu^+ \mu^-)/d\hat{s}$ , which show the RPV contributions distinguishable only in the high  $\hat{s}$  region.

As known, to probe new physics effects, it would be very useful to measure correlative observables, for example,  $\mathcal{B}(B_u^+ \rightarrow \rho^+ \ell^+ \ell^-)$ ,  $\mathcal{B}(B_u^+ \rightarrow \pi^+ \ell^+ \ell^-)$ , and  $\mathcal{B}(B_d \rightarrow \ell^+ \ell^-)$ , since correlations among these observables could provide very strict bound on new physics models.

It should be noted that the present upper limit of  $\mathcal{B}(B_u^+ \rightarrow \pi^+ \ell^+ \ell^-) < 9.1 \times 10^{-8}$  made by BABAR [15] is based on just  $208.9 \text{ fb}^{-1}$  data, which is already just one order higher than the SM expectation. Up to this Fall, Belle and BABAR have recorded as much as  $709 \text{ fb}^{-1}$  and  $500 \text{ fb}^{-1}$  data, respectively. Searches with these data will surely improve the upper limits for these decays to large extent, which will give much stronger constraints on the RPV SUSY parameter spaces. On the other hand, the decays with enhancement of the RPV SUSY might be accessible at BABAR and Belle, especially, the  $B_u^+ \rightarrow \rho^+ \ell^+ \ell^-$  decay. For such a measurement, a good  $\rho^+ \rightarrow \pi^+ \pi^0$  subvertex reconstruction is necessary to distinguish it from the much more copious decay  $B^+ \rightarrow K^{*+} \ell^+ \ell^- \rightarrow (K^+ \pi^0) \ell^+ \ell^-$ , and may be a challenging task at BABAR and Belle. In the near future at the LHCb, these decays might be measured with much larger data samples.

#### IV. SUMMARY

We have studied  $B_u^+ \rightarrow \pi^+ \ell^+ \ell^-$ ,  $B_u^+ \rightarrow \rho^+ \ell^+ \ell^-$ , and  $B_d^0 \rightarrow \ell^+ \ell^-$  decays extensively in the RPV SUSY. From the latest experimental upper limits of  $\mathcal{B}(B_u^+ \rightarrow \pi^+ \ell^+ \ell^-)$  and  $\mathcal{B}(B_d^0 \rightarrow \ell^+ \ell^-)$ , we have obtained the constrained parameter spaces of the RPV coupling products, and found these constraints are robust and stronger than the existing ones, which may be useful for further studies of the RPV SUSY phenomenology. Using the constrained parameter space, we have given the RPV impacts on the branching ratios  $\mathcal{B}(B_d^0 \rightarrow \ell^+ \ell^-)$ ,  $\mathcal{B}(B_u^+ \rightarrow \pi^+ \ell^+ \ell^-)$ , and  $\mathcal{B}(B_u^+ \rightarrow \rho^+ \ell^+ \ell^-)$ , and the forward-backward asymmetries  $\mathcal{A}_{\text{FB}}(B_u^+ \rightarrow \pi^+ \ell^+ \ell^-)$  and  $\mathcal{A}_{\text{FB}}(B_u^+ \rightarrow \rho^+ \ell^+ \ell^-)$ .

It is shown that  $\mathcal{B}(B_d^0 \rightarrow \ell^+ \ell^-)$  is very sensitive to the RPV  $s$ -channel sneutrino exchange, but not to  $t$ -channel squark exchange, which could be enhanced to  $\sim 10^{-8}$  by the former. On the contrary,  $B_u^+ \rightarrow \rho^+ \ell^+ \ell^-$  is very sensitive to  $t$ -channel squark exchange, and  $\mathcal{B}(B_u^+ \rightarrow \rho^+ \ell^+ \ell^-)$

could be enhanced to  $\sim 10^{-6}$ , which could be tested at *BABAR* and Belle.

Furthermore, we have shown the RPV effects on dilepton invariant mass spectra and the normalized forward-backward asymmetries in  $B_u^+ \rightarrow \pi^+ \ell^+ \ell^-$  and  $B_u^+ \rightarrow \rho^+ \ell^+ \ell^-$  decays. In the constrained parameter space, it is found that the RPV couplings  $\lambda'_{1i3} \lambda_{1i1}^*$  and  $\lambda'_{2i3} \lambda_{2i1}^*$  of squark exchanges could result in the distributions of  $d\mathcal{B}(B_u^+ \rightarrow \rho^+ \ell^+ \ell^-)/d\hat{s}$  and  $d\mathcal{A}_{\text{FB}}(B_u^+ \rightarrow \rho^+ \ell^+ \ell^-)/d\hat{s}$  significantly different from the SM expectations. The other four RPV couplings due to the sneutrino exchanges give distinguishable contributions to  $d\mathcal{B}(B_u^+ \rightarrow \pi^+ \ell^+ \ell^-)/d\hat{s}$  at high  $\hat{s}$  region. But for the  $B_u^+ \rightarrow \rho^+ \ell^+ \ell^-$  decays, the sneutrino exchange contributions to  $d\mathcal{B}/d\hat{s}$  and  $d\mathcal{A}_{\text{FB}}/d\hat{s}$  are indistinguishable from the theoretical uncertainties.

With the operation of *B* factories, many measurements of rare *B* decays have put strong constraints on new physics scenarios beyond the SM. With the near future experiments at the LHCb, one can access many more rare decays with high statistics, which will give more stringent bounds on

the products of the RPV couplings. From measurement of the correlated decays, one may eventually establish indirect evidence for specified new physics model or rule it out.

The results in this paper could be useful for probing the RPV SUSY effects and will correlate strongly with searches for the direct RPV signals at future experiments. Negative experimental evidence for the deviations from the SM expectations in these decays would result in strong constraints on these RPV couplings.

## ACKNOWLEDGMENTS

This work is supported by the National Science Foundation under contract Nos. 10675039 and 10735080, and the NCET Program sponsored by the Ministry of Education, China, under No. NCET-04-0656. The work of Ru-Min Wang is supported by the KRF Grant funded by the Korean Government (MOEHRD) No. KRF-2005-070-C00030.

- 
- [1] N. G. Deshpande *et al.*, Phys. Rev. Lett. **57**, 1106 (1986).  
 [2] B. Grinstein, M. J. Savage, and M. B. Wise, Nucl. Phys. **B319**, 271 (1989).  
 [3] A. J. Buras and M. Münz, Phys. Rev. D **52**, 186 (1995).  
 [4] W. Jaus and D. Wyler, Phys. Rev. D **41**, 3405 (1990).  
 [5] A. Ali *et al.*, Phys. Rev. D **55**, 4105 (1997); A. Ali and G. Hiller, Phys. Rev. D **58**, 071501 (1998); **58**, 074001 (1998).  
 [6] A. Ali *et al.*, Phys. Rev. D **61**, 074024 (2000).  
 [7] Y. B. Dai, C. S. Huang, and H. W. Huang, Phys. Lett. B **390**, 257 (1997); C. S. Huang *et al.*, Phys. Rev. D **63**, 114021 (2001).  
 [8] E. O. Iltan and G. Turan, Phys. Rev. D **63**, 115007 (2001).  
 [9] E. Lunghi *et al.*, Nucl. Phys. **B568**, 120 (2000); C. S. Huang and X. H. Wu, Nucl. Phys. **B657**, 304 (2003); S. R. Choudhury *et al.*, Phys. Rev. D **69**, 054018 (2004).  
 [10] Y. G. Xu, R. M. Wang, and Y. D. Yang, Phys. Rev. D **74**, 114019 (2006).  
 [11] B. Aubert *et al.* (*BABAR* Collaboration), Phys. Rev. D **73**, 092001 (2006).  
 [12] A. Ishikawa *et al.* (Belle Collaboration), Phys. Rev. Lett. **96**, 251801 (2006); K. Abe *et al.* (Belle Collaboration), arXiv:hep-ex/0410006.  
 [13] B. Aubert *et al.* (*BABAR* Collaboration), Phys. Rev. Lett. **98**, 151802 (2007).  
 [14] D. Mohapatra *et al.* (Belle Collaboration), Phys. Rev. Lett. **96**, 221601 (2006).  
 [15] B. Aubert *et al.* (*BABAR* Collaboration), Phys. Rev. Lett. **99**, 051801 (2007).  
 [16] A. J. Weir *et al.*, Phys. Rev. D **41**, 1384 (1990); K. W. Edwards *et al.* (CELO Collaboration), Phys. Rev. D **65**, 111102 (2002).  
 [17] D. Tonelli (CDF Collaboration), arXiv:hep-ex/0605038; P. Mack (CDF Collaboration), arXiv:hep-ex/0710.2502.  
 [18] F. Kruger and L. M. Sehgal, Phys. Rev. D **56**, 5452 (1997); **60**, 099905(E) (1999).  
 [19] T. M. Aliev and M. Savci, Phys. Rev. D **60**, 014005 (1999).  
 [20] E. O. Iltan, Int. J. Mod. Phys. A **14**, 4365 (1999).  
 [21] G. Erkol and G. Turan, J. High Energy Phys. 02 (2002) 015; Eur. Phys. J. C **25**, 575 (2002); G. Erkol, J. W. Wagenaar, and G. Turan, Eur. Phys. J. C **41**, 189 (2005).  
 [22] D. A. Demir, K. A. Olive, and M. B. Voloshin, Phys. Rev. D **66**, 034015 (2002); S. R. Choudhury and N. Gaur, Phys. Rev. D **66**, 094015 (2002).  
 [23] P. Fayet, Phys. Lett. **69B**, 489 (1977); G. R. Farrar and P. Fayet, Phys. Lett. **76B**, 575 (1978); N. Sakai and T. Yanagida, Nucl. Phys. **B197**, 533 (1982); C. S. Aulakh and R. N. Mohapatra, Phys. Lett. **119B**, 136 (1982).  
 [24] S. Weinberg, Phys. Rev. D **26**, 287 (1982).  
 [25] For recent reviews on RPV see, for example, R. Barbier *et al.*, Phys. Rep. **420**, 1 (2005), and references therein; M. Chemtob, Prog. Part. Nucl. Phys. **54**, 71 (2005).  
 [26] G. Bhattacharyya and A. Raychaudhuri, Phys. Rev. D **57**, R3837 (1998); D. Guetta, Phys. Rev. D **58**, 116008 (1998); G. Bhattacharyya and A. Datta, Phys. Rev. Lett. **83**, 2300 (1999); G. Bhattacharyya, A. Datta, and A. Kundu, Phys. Lett. B **514**, 47 (2001); D. Chakraverty and D. Choudhury, Phys. Rev. D **63**, 075009 (2001); **63**, 112002 (2001); D. Choudhury, B. Dutta, and A. Kundu, Phys. Lett. B **456**, 185 (1999); G. Bhattacharyya, A. Datta, and A. Kundu, J. Phys. G **30**, 1947 (2004); B. Dutta, C. S. Kim, and S. Oh, Phys. Rev. Lett. **90**, 011801 (2003); A. Datta, Phys. Rev. D **66**, 071702 (2002); C. Dariescu *et al.*, Phys. Rev. D **69**, 112003 (2004); S. Bar-Shalom, G. Eilam, and Y. D. Yang, Phys. Rev. D **67**, 014007 (2003); Y. D. Yang, R. M. Wang, and G. R. Lu, Phys. Rev. D **72**, 015009 (2005); **73**, 015003

- (2006); Ru-Min Wang *et al.*, Eur. Phys. J. C **47**, 815 (2006); J. H. Jang, J. K. Kim, and J. S. Lee, Phys. Rev. D **55**, 7296 (1997); J. P. Saha and A. Kundu, Phys. Rev. D **66**, 054021 (2002).
- [27] P. Ball and R. Zwicky, Phys. Rev. D **71**, 014015 (2005); **71**, 014029 (2005).
- [28] W. M. Yao *et al.* (Particle Data Group), J. Phys. G **33**, 1 (2006).
- [29] F. Krüger and L. M. Sehgal, Phys. Rev. D **55**, 2799 (1997).
- [30] G. Buchalla, A. Buras, and M. Lautenbacher, Rev. Mod. Phys. **68**, 1125 (1996).
- [31] M. Jezabek and J. H. Kühn, Nucl. Phys. **B320**, 20 (1989).
- [32] M. Misiak, Nucl. Phys. **B393**, 23 (1993); **B439**, 461(E) (1995).
- [33] N. G. Deshpande, J. Trampetić, and K. Panrose, Phys. Rev. D **39**, 1461 (1989); C. S. Lim, T. Morozumi, and A. I. Sanda, Phys. Lett. B **218**, 343 (1989).
- [34] A. I. Vainshtein *et al.*, Yad. Fiz. **24**, 820 (1976) [Sov. J. Nucl. Phys. **24**, 427 (1976)]; P. J. O'Donnell and H. K. Tung, Phys. Rev. D **43**, R2067 (1991).
- [35] K. S. Babu, K. R. S. Balaji, and I. Schienbein, Phys. Rev. D **68**, 014021 (2003).
- [36] S. Rai Choudhury, Phys. Rev. D **56**, 6028 (1997); C. S. Kim, T. Morozumi, and A. I. Sanda, Phys. Rev. D **56**, 7240 (1997); A. Ali and G. Hiller, Eur. Phys. J. C **8**, 619 (1999); hep-ph/9812267; H. M. Asatrian *et al.*, Phys. Rev. D **69**, 074007 (2004); T. M. Aliev, V. Bashiry, and M. Savci, Eur. Phys. J. C **31**, 511 (2003).
- [37] A. Ali, T. Mannel, and T. Morozumi, Phys. Lett. B **273**, 505 (1991).
- [38] G. Buchalla and A. J. Buras, Nucl. Phys. **B400**, 225 (1993).
- [39] J. Charles *et al.* (CKMfitter Group), Eur. Phys. J. C **41**, 1 (2005); updated results as of winter 2007 (Moriond07 and FPCP07) available at: <http://ckmfitter.in2p3.fr>.
- [40] A. Gray *et al.* (HPQCD Collaboration), Phys. Rev. Lett. **95**, 212001 (2005).
- [41] B. Aubert *et al.* (BABAR Collaboration), Phys. Rev. Lett. **94**, 221803 (2005).
- [42] H. K. Dreiner, M. Kramer, and Ben O'leary, Phys. Rev. D **75**, 114016 (2007).